quantities of LM/LAM (Fig. 8). Overexpression of MSMEG_4247 resulted in the production of dwarfed LM/LAM. In contrast, the deletion of MSMEG_4247 resulted in the disappearance of LM and accumulation of branchless LAM. We suggest that overexpression of the branching mannosyltransferase results in premature chain termination, whereas in the absence of branching, transiently synthesized branchless LM is either converted to LAM or degraded. Below, we discuss possible control mechanisms of mannan chain length and why branchless LM cannot be stably maintained.

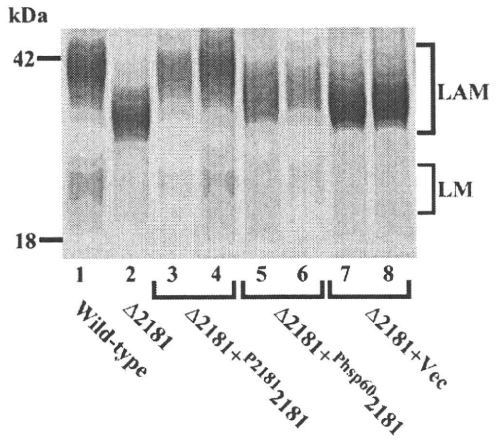


FIGURE 7. **LM/LAM profiles of *M. tuberculosis Rv2181* deletion mutants transfected with various expression vectors.** LM/LAM were extracted, analyzed by SDS-PAGE, and visualized by carbohydrate staining. *Lane 1*, wild type; *lane 2*, Δ*Rv2181* mutant; *lanes 3* and *4*, Δ*Rv2181* mutant transfected with pYAB228, an integrative expression vector carrying *Rv2181*, including 242 bp of upstream sequence; *lanes 5* and *6*, Δ*Rv2181* mutant transfected with pYAB230, an integrative expression vector carrying *Rv2181* driven by Phsp60; *lanes 7* and *8*, Δ*Rv2181* mutant transfected with pYAB184, an integrative empty vector control.

Most important, the following two pieces of evidence suggested that MSMEG_4247 affects the sizes of LM/LAM primarily by competing with the elongating α1,6-mannosyltransferase. First, we showed that 15-fold or more overexpression of MSMEG_4247 resulted in short α1,6-mannose backbone (see Figs. 2 and 3). Second, overexpression of elongating α1,6-mannosyltransferase (MSMEG_4241) alleviated the dwarfing effect of MSMEG_4247 overexpression (see Fig. 5). Dwarfed LM/LAM are unlikely to be caused by substrate depletion because MSMEG_4241 overexpression can at least partially override the dwarfing effect of MSMEG_4247 overexpression. It is tempting to speculate that MSMEG_4241 and MSMEG_4247 compete for the growing non-reducing terminus of mannan polymer, and MSMEG_4247-mediated α1,2-mannosylation of the non-reducing end blocks further elongation. Future studies using a cell-free assay system and synthetic substrates will address these possibilities.

Interestingly, overexpression of MSMEG_4247 resulted in the dwarfing of not only the mannan chain but the arabinan moiety of LAM (see Fig. 2*E*). Because both MSMEG_4241 and MSMEG_4247 are mannosyltransferases, it is unclear how the expression levels of these enzymes affect the arabinan size. One possibility is that multiple arabinans are attached to a single LAM molecule, and a short mannan chain limits the sites available for arabinosylation. In another experiment, we showed that overexpressed MSMEG_4241 competed with overexpressed MSMEG_4247 in terms of the LAM mannan size, but the restoration of the arabinan size was only partial (see Fig. 5). We speculate that relatively low (wild-type) expression levels of arabinosyltransferases compared with overexpressed mannosyltransferases have led to the reduction in arabinan size. Based on these observations, it is conceivable that the expression levels of arabinosyltransferases are also controlled in concert with the two mannosyltransferases to coordinate LAM synthesis in wild-type cells. Identification and characterization of the arabinosyltransferase that initiates the arabinan synthesis will provide further mechanistic insight into LAM biosynthesis.

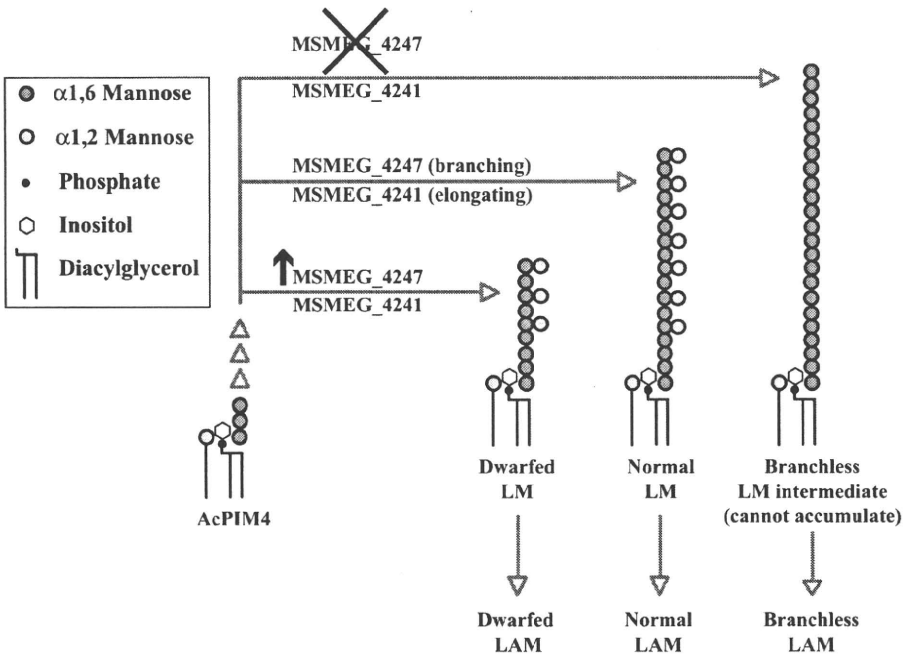


FIGURE 8. **A model of LM/LAM biosynthesis involving elongating (MSMEG_4241) and branching (MSMEG_4247) mannosyltransferases.** The lack of MSMEG_4247 results in the lack of LM and accumulation of branchless LAM. In contrast, overexpression of MSMEG_4247 results in dwarfed LM and dwarfed LAM. The positions of α1,2-mannose branches are hypothetical. Although our data are consistent with LM being a precursor of LAM biosynthesis, the precursor-product relationship of LM and LAM remains to be proved. The structure of LM intermediate in Δ*MSMEG_4247* mutant is hypothetical, based on the structure of LAM accumulating in the mutant.

The lack of α1,2-monomannose branching resulted in the complete absence of LM in both *M. smegmatis* and *M. tuberculosis* (see Figs. 1*B* and 7) (22), suggesting a conserved function of α1,2-mannose branching in LM accumulation. There are

several possibilities for why branchless LM cannot accumulate. First, in the absence of branching-dependent chain termination, MSMEG_4241 may be incapable of terminating the mannan polymerization by itself. We then speculate that arabinosylation acts as an alternative termination signal, thus resulting in the production of LAM only. Second, contrary to the first possibility, MSMEG_4241 may be able to terminate the polymer elongation after reaching a certain chain length, producing branchless LM. However, branchless LM cannot accumulate stably, perhaps because it is either efficiently converted to LAM or degraded. These possibilities are not exclusive to each other, and in either case, there appears to be an alternative chain termination mechanism in addition to mannose branching to control the mannan chain length. We consistently observed more enriched accumulation of branchless LAM in the Δ*MSMEG_4247* mutant compared with the wild-type levels. Although the precursor-product relationship of LM and LAM is not established, this observation favors the possibility that branchless LM intermediate is more avidly converted to LAM rather than being degraded. Curiously, although our *M. tuberculosis* Δ*Rv2181* mutant showed a complete lack of LM, another recently reported Δ*Rv2181* mutant accumulated small size LM (23). Further studies are necessary to identify factors that have led these two Δ*Rv2181* mutants into different phenotypes.

At least a fraction of LAM synthesized in the plasma membrane appears to be transported to the surface layer of the cell wall (34), suggesting a dynamic spatial control of LAM biosynthesis. We demonstrated that both MSMEG_4247 and MSMEG_4241 are topologically confined in a membrane domain known as PM-CW (see Fig. 6, *A–C*), suggesting that LAM is synthesized in a spatially controlled manner, and these two enzymes may function in topological proximity. If MSMEG_4247 and MSMEG_4241 form a heterodimer, overexpression of kinetically inactive MSMEG_4247 may interfere with the formation of a functional dimer in the wild-type cells, leading to a phenotype similar to Δ*MSMEG_4247* mutant. However, such dominant negative effects were not observed (see Fig. 3*A*), making heterodimer formation less likely. We do not know if the levels of overexpression achieved in this study occur in physiological situations. Nevertheless, our results suggest that the expression levels of MSMEG_4247 and MSMEG_4241 need to be controlled in concert to avoid the production of aberrant LM/LAM. Being consistent with this suggestion, disappearance of LM/LAM in the stationary phase was closely correlated with concerted down-regulation of both enzymes (see Fig. 6, *D* and *E*). Interestingly, truncated structural variants of LAM have been identified in *Mycobacterium leprae* and clinical isolates of *M. tuberculosis* (33), implying that the polymer length of LM/LAM can vary among species/strains and may be controlled in response to environmental stimuli. Controlling the expression levels of MSMEG_4247 and MSMEG_4241 in *M. smegmatis* or their orthologs in other species may represent a key feature of the polymer length control of mycobacterial LM/LAM. Understanding the mechanisms of transcriptional and post-transcriptional controls of MSMEG_4247 and MSMEG_4241 expressions may provide further clues to understand the regulatory mechanisms of LM/LAM biosynthesis.

*Acknowledgments—We thank Hidekazu Murakami, Dr. Morihisa Fujita, and Dr. Matthew Stokes for critical reading of the manuscript, Keiko Kinoshita for technical assistance, Dr. William R. Jacobs, Jr. (Albert Einstein College of Medicine) for kindly providing vectors pMV306 and pMV361, and Dr. Helen Billman-Jacobe (University of Melbourne) for kindly providing pJAM2 vector.*

## REFERENCES

1. Brennan, P. J. (2003) *Tuberculosis* **83,** 91–97
2. Briken, V., Porcelli, S. A., Besra, G. S., and Kremer, L. (2004) *Mol. Microbiol.* **53,** 391–403
3. Alderwick, L. J., Birch, H. L., Mishra, A. K., Eggeling, L., and Besra, G. S. (2007) *Biochem. Soc. Trans.* **35,** 1325–1328
4. Khoo, K. H., Dell, A., Morris, H. R., Brennan, P. J., and Chatterjee, D. (1995) *Glycobiology* **5,** 117–127
5. Lee, Y. C., and Ballou, C. E. (1964) *J. Biol. Chem.* **239,** 1316–1327
6. Brennan, P., and Ballou, C. E. (1967) *J. Biol. Chem.* **242,** 3046–3056
7. Khoo, K. H., Douglas, E., Azadi, P., Inamine, J. M., Besra, G. S., Mikusová, K., Brennan, P. J., and Chatterjee, D. (1996) *J. Biol. Chem.* **271,** 28682–28690
8. Kaur, D., McNeil, M. R., Khoo, K. H., Chatterjee, D., Crick, D. C., Jackson, M., and Brennan, P. J. (2007) *J. Biol. Chem.* **282,** 27133–27140
9. Chatterjee, D., Hunter, S. W., McNeil, M., and Brennan, P. J. (1992) *J. Biol. Chem.* **267,** 6228–6233
10. Shi, L., Berg, S., Lee, A., Spencer, J. S., Zhang, J., Vissa, V., McNeil, M. R., Khoo, K. H., and Chatterjee, D. (2006) *J. Biol. Chem.* **281,** 19512–19526
11. Besra, G. S., Morehouse, C. B., Rittner, C. M., Waechter, C. J., and Brennan, P. J. (1997) *J. Biol. Chem.* **272,** 18460–18466
12. Brennan, P., and Ballou, C. E. (1968) *J. Biol. Chem.* **243,** 2975–2984
13. Morita, Y. S., Patterson, J. H., Billman-Jacobe, H., and McConville, M. J. (2004) *Biochem. J.* **378,** 589–597
14. Guerin, M. E., Kaur, D., Somashekar, B. S., Gibbs, S., Gest, P., Chatterjee, D., Brennan, P. J., and Jackson, M. (2009) *J. Biol. Chem.* **284,** 25687–25696
15. Korduláková, J., Gilleron, M., Mikusova, K., Puzo, G., Brennan, P. J., Gicquel, B., and Jackson, M. (2002) *J. Biol. Chem.* **277,** 31335–31344
16. Korduláková, J., Gilleron, M., Puzo, G., Brennan, P. J., Gicquel, B., Mikusová, K., and Jackson, M. (2003) *J. Biol. Chem.* **278,** 36285–36295
17. Morita, Y. S., Sena, C. B., Waller, R. F., Kurokawa, K., Sernee, M. F., Nakatani, F., Haites, R. E., Billman-Jacobe, H., McConville, M. J., Maeda, Y., and Kinoshita, T. (2006) *J. Biol. Chem.* **281,** 25143–25155
18. Crellin, P. K., Kovacevic, S., Martin, K. L., Brammananth, R., Morita, Y. S., Billman-Jacobe, H., McConville, M. J., and Coppel, R. L. (2008) *J. Bacteriol.* **190,** 3690–3699
19. Kovacevic, S., Anderson, D., Morita, Y. S., Patterson, J., Haites, R., McMillan, B. N., Coppel, R., McConville, M. J., and Billman-Jacobe, H. (2006) *J. Biol. Chem.* **281,** 9011–9017
20. Mishra, A. K., Alderwick, L. J., Rittmann, D., Tatituri, R. V., Nigou, J., Gilleron, M., Eggeling, L., and Besra, G. S. (2007) *Mol. Microbiol.* **65,** 1503–1517
21. Mishra, A. K., Alderwick, L. J., Rittmann, D., Wang, C., Bhatt, A., Jacobs, W. R., Jr., Takayama, K., Eggeling, L., and Besra, G. S. (2008) *Mol. Microbiol.* **68,** 1595–1613
22. Kaur, D., Berg, S., Dinadayala, P., Gicquel, B., Chatterjee, D., McNeil, M. R., Vissa, V. D., Crick, D. C., Jackson, M., and Brennan, P. J. (2006) *Proc. Natl. Acad. Sci. U.S.A.* **103,** 13664–13669
23. Kaur, D., Obregón-Henao, A., Pham, H., Chatterjee, D., Brennan, P. J., and Jackson, M. (2008) *Proc. Natl. Acad. Sci. U.S.A.* **105,** 17973–17977
24. Snapper, S. B., Lugosi, L., Jekkel, A., Melton, R. E., Kieser, T., Bloom, B. R., and Jacobs, W. R., Jr. (1988) *Proc. Natl. Acad. Sci. U.S.A.* **85,** 6987–6991
25. Haites, R. E., Morita, Y. S., McConville, M. J., and Billman-Jacobe, H. (2005) *J. Biol. Chem.* **280,** 10981–10987
26. Stover, C. K., de la Cruz, V. F., Fuerst, T. R., Burlein, J. E., Benson, L. A., Bennett, L. T., Bansal, G. P., Young, J. F., Lee, M. H., and Hatfull, G. F. (1991) *Nature* **351,** 456–460
27. Triccas, J. A., Parish, T., Britton, W. J., and Gicquel, B. (1998) *FEMS Mi-*

*crobiol. Lett.* **167,** 151–156
28. Schneider, P., Ralton, J. E., McConville, M. J., and Ferguson, M. A. (1993) *Anal. Biochem.* **210,** 106–112
29. Sauton, B. (1912) *C. R. Acad. Sci. III* **155,** 860–863
30. Morita, Y. S., Velasquez, R., Taig, E., Waller, R. F., Patterson, J. H., Tull, D., Williams, S. J., Billman-Jacobe, H., and McConville, M. J. (2005) *J. Biol. Chem.* **280,** 21645–21652
31. Khoo, K. H., Dell, A., Morris, H. R., Brennan, P. J., and Chatterjee, D. (1995) *J. Biol. Chem.* **270,** 12380–12389
32. Gilleron, M., Himoudi, N., Adam, O., Constant, P., Venisse, A., Rivière, M., and Puzo, G. (1997) *J. Biol. Chem.* **272,** 117–124
33. Torrelles, J. B., Khoo, K. H., Sieling, P. A., Modlin, R. L., Zhang, N., Marques, A. M., Treumann, A., Rithner, C. D., Brennan, P. J., and Chatterjee, D. (2004) *J. Biol. Chem.* **279,** 41227–41239
34. Pitarque, S., Larrouy-Maumus, G., Payré, B., Jackson, M., Puzo, G., and Nigou, J. (2008) *Tuberculosis* **88,** 560–565

International Immunology, Vol. 22, No. 3, pp. 179–189
doi:10.1093/intimm/dxp126
Advance Access publication 5 February 2010



# Transient role of $CD4^+CD25^+$ regulatory T cells in mycobacterial infection in mice

**Yuriko Ozeki[1,2], Isamu Sugawara[3], Tadashi Udagawa[3], Toshiaki Aoki[3], Mayuko Osada-Oka[1], Yoshitaka Tateishi[1], Hajime Hisaeda[4], Yuji Nishiuchi[5], Nobuyuki Harada[3], Kazuo Kobayashi[6] and Sohkichi Matsumoto[1]**

[1]Department of Bacteriology, Osaka City University Graduate School of Medicine, 1-4-3 Abeno-ku, Osaka 545-8585, Japan
[2]Sonoda Women's University, 7-29-1 Minamitsukaguchi-cho, Amagasaki, Hyogo 661-8520, Japan
[3]Mycobacterial Reference Center, The Research Institute of Tuberculosis, 3-1-24 Matsuyama Kiyose-shi Tokyo, 204-8533, Japan
[4]Department of Microbiology and Immunology, Graduate School of Medical Sciences, Kyushu University, 3-1-1 Maidashi, Higashi-ku, Fukuoka 812-8582, Japan
[5]Peptide Institute Inc., Protein Research Foundation, Minoh-shi, Osaka 562-8686, Japan
[6]Department of Immunology, National Institute of Infectious Diseases, Toyama 1-23-1, Shinjuku-ku, Tokyo 162-8640, Japan

*Correspondence to*: S. Matsumoto and Y. Ozeki; E-mail. sohkichi@med.osaka-cu.ac.jp and yuriozeki@med.osaka-cu.ac.jp

*Transmitting editor*: S. Koyasu

*Received* 22 April 2009, *accepted* 22 December 2009

**Abstract**

**$CD4^+CD25^+$ regulatory T (Treg) cells cause immune suppression by inhibiting T cell effector functions and play pivotal roles not only in self-tolerance but also in immune response to parasitic microbial pathogens. Mycobacteria are major parasitic bacterial pathogens, but the role of $CD4^+CD25^+$ Treg cells in mycobacterial infection is not yet defined. In this study we found that, at the early stage of infection, depletion of $CD25^+$ cells reduced both bacterial load and granuloma formation in mice infected with *Mycobacterium tuberculosis* strains, such as *M. tuberculosis* Erdman or *M. tuberculosis* Kurono. However, at a later stage of infection, bacterial burden and histopathology were similar regardless of depletion of $CD25^+$ cells. Severe combined immunodeficient (SCID) mice reconstituted with $CD4^+CD25^-$ T cells alone or a combination of $CD4^+CD25^+$ and $CD4^+CD25^-$ T cells showed similar bacterial loads and survival kinetics after infection with *M. tuberculosis* Erdman. Consistent with *in vivo* data, *in vitro* studies revealed that mycobacterial antigens, purified protein derivative of tuberculin (PPD), failed to induce the suppressive function of $CD4^+CD25^+$ Treg cells to $CD4^+CD25^-$ effector T cells, as demonstrated by the lack of response of $CD4^+CD25^+$ T cells to PPD, in mice chronically infected with *Mycobacterium bovis* bacillus Calmette–Guérin and *M. tuberculosis*. Our data show that $CD4^+CD25^+$ Treg cells have a transient effect at the early stage of mycobacterial infection but, contrary to the expectation, have little impact on the overall course of infection.**

*Keywords*: bacterial, T cells, rodent, inflammation, lung

## Introduction

Mycobacteria are intracellular bacterial pathogens, which persistently infect eukaryotes, including mammals, and cause diseases not only following primary infection but also by reactivation from latent state. Several species of mycobacteria, such as *Mycobacterium tuberculosis* and *Mycobacterium bovis*, are known to cause human tuberculosis. The World Health Organization estimates that *M. tuberculosis* infects one-third of the world's population and is responsible for 2 million deaths each year (1). While the infection remains latent in 95% of the infected cases of *M. tuberculosis*, 5–10% of those who initially controlled the infection later develop active disease at some stage during their lifetime. To suppress intracellular growth of mycobacteria, macrophage activation by IFN-gamma is critical in both mice (2, 3) and humans (2, 3).

The important role of the $CD4^+CD25^+$ regulatory T (Treg) cells in immune response has recently been recognized. This T cell subset maintains immunologic self-tolerance and suppresses the onset of autoimmune diseases (4). The vast majority of Treg cells constitutively express CD25/IL-2 receptor alpha chain in the physiological state (5, 6). $CD4^+CD25^+$ Treg cells also express cytotoxic T-lymphocyte-associated protein 4 (CTLA-4; 7, 8), glucocorticoid-induced tumor necrosis factor receptor (GITR; 9, 10) and the transcription factor,

FoxP3 (11, 12). Some subsets of $CD4^+CD25^+$ Treg cells also produce effector cytokines, such as IL-10 and transforming growth factor (TGF)-β (13, 14). The defining feature of $CD4^+CD25^+$ Treg cells is their ability to inhibit the proliferation of T cells and IFN-gamma production through cell–cell contact (15, 16), possibly mediated by CTLA-4, and/or through the production of immunosuppressive cytokines, such as TGF-β and IL-10 (13, 14).

Recently, it has been reported that $CD4^+CD25^+$ Treg cells are also involved in suppressive immune responses during several infectious diseases. Depletion of $CD4^+CD25^+$ Treg cells enhances anti-microbial activity against diverse pathogens including the protozoan *Leishmania major* and *Plasmodium yoelii*, viruses such as HIV and Herpes simplex virus and bacteria such as *Helicobacter pylori* (17–21).

In spite of suggested importance of $CD4^+CD25^+$ Treg cells in parasitic pathogens, the knowledge in mycobacterial infection remains controversial (22–25). Kursar *et al.* and Scott-Browne *et al.* showed that Treg cells prevented protective immunity against *M. tuberculosis* infection by utilizing reconstituted and chimeric mice, respectively (22, 25). In contrast, Quinn *et al.* suggested minor role of $CD4^+CD25^+$ in both *Mycobacterium bovis* bacillus Calmette Guérin (BCG)-induced protection and natural mycobacterial infection (23, 24). In order to elucidate the roles of $CD4^+CD25^+$ Treg cells in mycobacterial infection more precisely, we carried out the experiments using Treg-deleted mice by antibody to CD25 molecule and SCID mice reconstituted with T cell subsets. We found that mycobacterial antigen-specific $CD4^+CD25^+$ Treg cells were hardly developed after mycobacterial infection in mice and therefore the function of $CD4^+CD25^+$ Treg cells was limited after the infection was established. Thus, $CD4^+CD25^+$ Treg cells have little impact on the overall course of mycobacterial infection.

## Methods

### *Mice*

Specific pathogen-free, female DBA/2 mice aged 6 weeks were purchased from Japan SLC (Shizuoka, Japan). BALB/c and SCID/BALB/c mice were purchased from Japan CLEA (Tokyo, Japan). All mice were maintained under specific pathogen-free conditions in the animal facilities of Osaka City University Graduate School of Medicine and in a biosafety-level-3 facility at The Research Institute of Tuberculosis according to the standard guidelines for animal experiments at each institute with approval of their ethical committees.

### *Depletion of $CD4^+CD25^+$ cells*

A hybridoma cell line expressing anti-mouse CD25 monoclonal IgM [a monoclonal antibody against mouse CD25 (7D4), American Type Culture Collection, Manassas, VA, USA] was expanded as ascites in pristine-primed SCID mice (Wako, Osaka, Japan). The Ig-rich fraction was obtained by 30% ammonium sulfate precipitation of ascitic fluid followed by dialysis in PBS. An isotype-matched control IgM was purchased from eBioscience (San Diego, CA, USA). The protein concentration was determined by Bradford's method using BSA (Sigma–Aldrich, St Louis, MO, USA) as a standard. For depletion of $CD25^+$ cells in early stage of infection, mice were injected with 1 mg of 7D4 or control IgM intraperitoneally (i.p.) 1 day before, and then 3 and 10 days after *M. tuberculosis* infection. For depletion of $CD25^+$ cells in late stage of infection, mice were injected (i.p.) with 1 mg of 7D4 or control IgM at 60, 65 and 70 days after *M. tuberculosis* infection. Depletion of $CD4^+CD25^+$ cells was assessed by flow cytometry using a FACScan (Becton Dickinson, Franklin Lakes, NJ, USA). Peripheral blood leukocytes (PBLs) were obtained by incubation with 0.83% ammonium chloride solution at 37°C for 5 min to induce erythrocyte lysis. PBLs or splenocytes were stained with PE-conjugated anti-CD4 mAb (GK1.5, eBioscience) and FITC-conjugated anti-CD25 mAb (PC61, eBioscience). The data were analyzed by flow cytometry with using Cellquest™ software (Becton Dickinson).

### *Bacteria and infection*

*Mycobacterium bovis* BCG Tokyo, *M. tuberculosis* H37Rv, *M. tuberculosis* Kurono (ATCC 35812) and *M. tuberculosis* Erdman were grown in 7H9 medium (Difco, Detroit, MI, USA) supplemented with 10% BSA, dextrose and catalase enrichment (Difco) and 0.05% Tween 80 at 37°C to mid-logarithmic phase, then stored in frozen aliquots as previously described (26). For infection with *M. tuberculosis* Kurono and *M. tuberculosis* Erdman, the nebulizer of a Middlebrook airborne infection apparatus (Glas-col, Terre Haute, IN, USA) was filled with 5 ml PBS containing $5 \times 10^6$ colony-forming units (CFU) of bacteria and the mice were airborne infected for 90 min by Glas-Col aerosol generator. This procedure deposits ~10 CFU of bacteria into the lungs. At 0, 3 and 5 weeks (and also 2 weeks in some experiments) post-infection, three to five mice per group were euthanized and the lungs, livers and spleens were harvested. The organs were homogenized in 1 ml sterile distilled water using a mortar and pestle and serial dilutions were plated onto Middlebrook 7H11 agar containing oleic acid, dextrose, albumin and catalase enrichment (Difco) (7H11-OADC agar). Bacterial numbers were counted using CFU after culturing at 37°C for 20–30 days. To investigate the role of $CD4^+CD25^+$ Treg cells in the late stage of infection, mice were airborne-infected with *M. tuberculosis* H37Rv as the same method described above and $CD25^+$ cells were depleted by 7D4 treatment on days 60, 65, and 70. At 75 days post-infection, eight mice per group were euthanized and bacterial numbers in lungs and spleens were determined by CFU count and histological evaluation were performed as the same procedures described above.

### *Isolation of $CD4^+CD25^+$ T cells and $CD4^+CD25^-$ T cells*

BALB/c mice were infected i.p. with $5 \times 10^4$ CFU of *M. bovis* BCG Tokyo. $CD4^+CD25^+$ T cells and $CD4^+CD25^-$ T cells were purified from spleens of normal mice or chronically BCG-infected (>6 months post-infection) BALB/c mice using $CD4^+CD25^+$ regulatory T cell isolation kit (Miltenyl Biotec, Bergisch Gladgach, Germany) after depleting erythrocytes with 0.83% ammonium chloride solution. Obtained cells were labeled with PE-conjugated anti-CD25 mAb, stained with FITC-conjugated anti-CD4 mAb (eBioscience) and analyzed

by flow cytometer. The purity of selected populations was confirmed as >96%. Expression of foxp3 in the $CD4^+CD25^+$ T cell population was confirmed using flow cytometer after intracellular staining with anti-FITC-conjugated anti-mouse foxp3 mAb (eBioscience). $CD4^+CD25^+$ T cells stained by this procedure were >90% foxp3-positive. Non-$CD4^+$ cells of normal mice retained in the MACS separation column were flushed out and incubated for >2 h. Attached cells were used as antigen-presenting cells (APCs) after treatment with 20-Gy radiation. T cell populations and APCs were also isolated from DBA/2 mice chronically infected with *M. tuberculosis* as the similar procedure with BCG-infected mice described above. However, in this case, to obtain APCs, spleen cells of normal DBA/2 mice were incubated for >2 h and attached cells were treated with mitomycin C (50 μg $zml^{-1}$) for 30 min at 37°C instead of radiation.

*In vitro T cell proliferation assay and measurement of cytokines*

$CD4^+CD25^+$ T cells and $CD4^+CD25^-$ T cells were prepared to be $1 \times 10^6$ cells $ml^{-1}$. Various ratios of $CD4^+CD25^+$ T cells and $CD4^+CD25^-$ T cells were cultured for 5 or 7 days with 10 μg $ml^{-1}$ of purified protein derivative of tuberculin (PPD) or anti-CD3 mAb (CEDARLANE, Canada) in the presence of $1 \times 10^5$ cells $ml^{-1}$ of APC in 96-well plates in RPMI 1640 supplemented with 10% FCS, 2 mM L-glutamine, penicillin (100 U $ml^{-1}$), streptomycin (100 mg $ml^{-1}$) and 50 mM 2-mercaptoethanol. Proliferation was evaluated by pulsing cells with 1 μCi (37 kBq) per well [$^3$H]thymidine ([$^3$H]TdR) for 6 h and [$^3$H]TdR incorporation measured using a scintillation counter. In the experiments to analyze the function of T cells derived from *M. tuberculosis*-infected mice, proliferation was evaluated by incorporation of 5-bromo-2′-deoxyuridine (BrdU) using a commercially available kit (Cell proliferation ELISA, BrdU colorimetoric, Roche, Germany). Production of IFN-gamma, IL-10, IL-2 and IL-6 in the culture supernatant was measured using a commercially available ELISA kit (R&D System, Minneapolis, MN, USA).

*Transfer of T cell population into SCID mice*

$CD4^+CD25^+$ T cells and $CD4^+CD25^-$ T cells were purified from the spleens of BALB/c mice chronically infected with BCG using $CD4^+CD25^+$ Treg cell isolation kit. Totally, $7.5 \times 10^5$ $CD4^+CD25^-$ T cells or $7.5 \times 10^5$ $CD4^+CD25^+$ T cells either alone or in combination ($7.5 \times 10^5$ $CD4^+CD25^-$ T cells and $7.5 \times 10^4$ $CD4^+CD25^+$ T cells) were transferred intravenously to cognate SCID mice (17). One day after transfer, recipient mice were infected aerogenically with *M. tuberculosis* Erdman as described above. Three weeks post-infection, five to eight mice were euthanized and bacterial burden was counted. The survival time course of seven mice per group was observed for up to 165 days post-infection.

*Neutralization of IL-6 in culture supernatant*

$CD4^+CD25^-$ T cells, $CD4^+CD25^+$ T cells and APCs were isolated from chronically BCG-infected mice according to the procedures described above. Anti-mouse IL-6-neutralizing mAb (Biolegend, San Diego, CA, USA) or isotype-matched control antibody (Southern Biotech, Birmingham, AL, USA) was added to the culture of $CD4^+CD25^-$ effector T cells either alone or in combination with $CD4^+CD25^+$ T cells at concentration of 0.02 μg $ml^{-1}$ and cultured for 4 days in the presence of PPD or anti-CD3 mAb. IFN-gamma production and [$^3$H]TdR incorporation were measured after 4 days incubation.

*Transfer of culture medium*

T cell subsets were obtained from chronically BCG-infected mice as described above. $CD4^+CD25^-$ T cells/$CD4^+CD25^+$ T cells/APCs (1:0:0.1) or $CD4^+CD25^-$ T cells/$CD4^+CD25^+$ T cells/APCs (1:1:0.1) were cultured with PPD or anti-CD3 mAb for 7 days and each culture supernatant stored at −80°C until later use. Freshly isolated $CD4^+CD25^-$ T cells/$CD4^+CD25^+$ cells/APCs (1:0:0.1) or $CD4^+CD25^-$ T cells/$CD4^+CD25^+$ T cells/APCs (1:1:0.1) were cultured with stored supernatant:new medium (1:1) in the presence or absence of anti-CD3 mAb. On day 4, [$^3$H]TdR incorporation was measured as described above.

*In vitro activation of $CD4^+CD25^+$ T cells*

$CD4^+CD25^+$ T cells isolated from chronically infected BALB/c mice with BCG or *M. tuberculosis* H37Rv were incubated with Dynabeads Mouse CD3/CD28 T cell Expander (Invitrogen, Norway) at a bead:cell ratio of 2:1 adding 2000 U $ml^{-1}$ of recombinant mouse IL-2 according to the manufacturer's protocol. Two days after incubation, the beads were

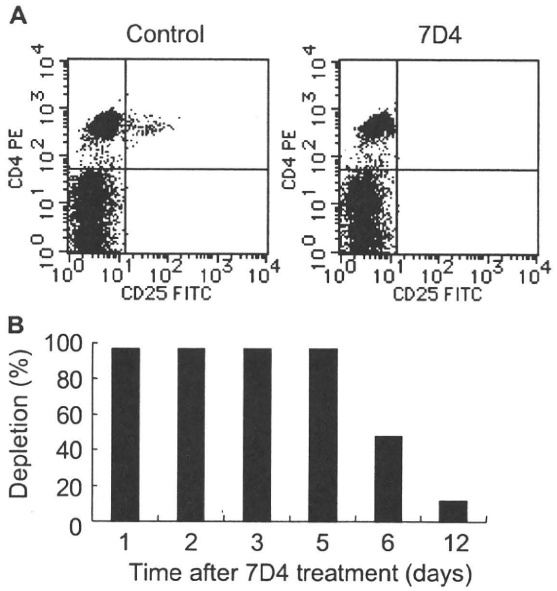


**Fig. 1.** Selective loss of $CD4^+CD25^+$ T cells by treatment with anti-CD25 mAb, 7D4. (A) Flow cytometric analysis of PBLs obtained from i.p.-injected mice with 1 mg of anti-CD25 mAb (7D4) or control IgM (control) 1 day after injection. Cells were stained with FITC-conjugated anti-CD25 mAb (PC61) and PE-conjugated anti-CD4 mAb (GK1.5). (B) Time course of the level of depletion of $CD4^+CD25^+$ T cell in PBL after a single dose of 7D4. Data are expressed as percent depleted relative to the $CD4^+CD25^+$ cell population in control IgM-treated mice. Data are mean of three mice per time point.

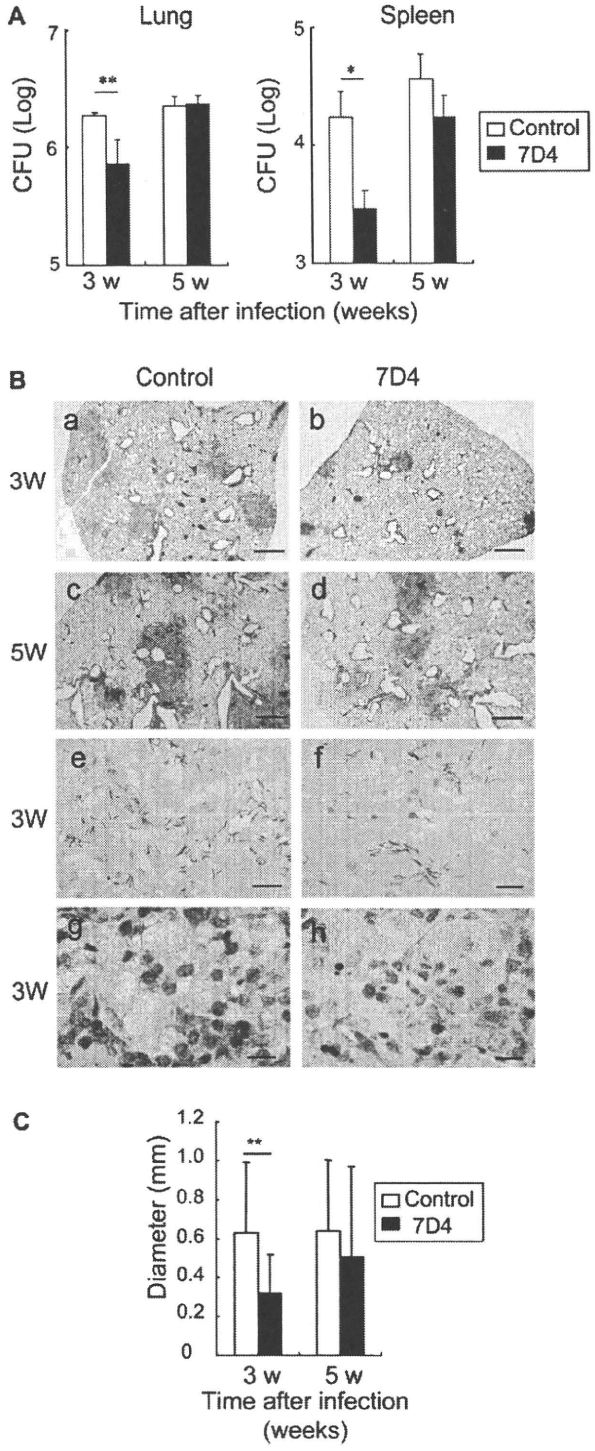


**Fig. 2.** The effect of $CD25^+$ cell depletion in *Mycobacterium tuberculosis* Kurono infection in mice. DBA/2 mice treated with 1 mg of 7D4, anti-CD25 mAb or control IgM were aerogenically infected with $5 \times 10^6$ CFU of *M. tuberculosis* Kurono. (A) Bacterial numbers were counted in lungs (left panel) and spleens (right panel) of mice treated with control IgM (open bars) or with 7D4, anti-CD25 mAb (closed bars). (B) Histopathological features of lungs from *M. tuberculosis* Kurono-infected mice. Lung sections were stained with H&E (a–d), Ziehl–Neelsen (e and f) and Giemsa (g and h). Granulomas mainly consisted of epithelioid macrophages (g and h). Numerous acid-fast bacteria were observed in granulomas of both control IgM-treated and anti-CD25 mAb-treated (7D4) mice. (a, c, e and g) Lungs sections from mice treated with control IgM. (b, d, f and h) Lungs sections from mice treated with 7D4. (a, b and e–h) Three weeks after infection. (c and d) Five weeks after infection. Bars, 500 μm (a–d), 10 μm (e-h). (C) The diameter of granulomatous lesions was measured in the lung sections from mice treated with control IgM (open bars) or with 7D4, anti-CD25 mAb (closed bars). Bars represent mean ±standard deviation of three to five mice. $*P < 0.05$ versus control mice; $**P < 0.01$ versus control mice.

removed from $CD4^+CD25^+$ T cells by magnet. After washing with medium, cells were used as activated $CD4^+CD25^+$ T cells. Freshly isolated $CD4^+CD25^-$ effector T cells were incubated with activated $CD4^+CD25^+$ T cells in the presence of PPD.

*Histological analysis*

Tissues were removed from mice at various intervals, fixed in 10% formalin and embedded in paraffin blocks. Sections (5 μm) were stained with hematoxylin and eosin (H&E), Ziehl–Neelsen or Giemsa methods. To evaluate the intensity of inflammatory response of the lung, the mean diameters of pulmonary granulomas were measured in three sections per mouse using Microanalyzer (Poladigital, Tokyo, Japan).

*Statistical analysis*

Results were analyzed by one-way analysis of variance (ANOVA) by SAS system R.8.1. Data were expressed as mean values ± standard deviation and considered significant if $P < 0.05$.

## Results

*Depletion of $CD25^+$ cells in early stage of infection causes transient effect on in vivo growth of M. tuberculosis Kurono and M. tuberculosis Erdman*

7D4 is a mAb against mouse CD25. Administration of 1 mg 7D4 into a mouse resulted in the loss of >96% of $CD4^+CD25^+$ T cells in the peripheral blood and spleens (Fig. 1A). Loss of $CD25^+$ cells maintained at least for 5 days after 7D4 treatment (Fig. 1B). Depletion of $CD25^+$ cells by 7D4 protects mice from death caused by infection of *Plasmodium yoelii*, suggesting a role for $CD4^+CD25^+$ Treg cells in exacerbating malaria (21).

Using 7D4, we first depleted $CD25^+$ cells of DBA/2 mice and then infected animals with $5 \times 10^6$ CFU/mouse of *M. tuberculosis* Kurono, which was clinically isolated strain in Japan, by airborne infection. Bacterial load in lung and spleen, and histopathology of the lung were monitored at 3 and 5 weeks post-infection. *Mycobacterium tuberculosis* Kurono multiplied to approximately $2 \times 10^6$ CFU per lung 3 weeks post-challenge and maintained these bacterial numbers 5 weeks post-challenge. In spleens, we detected $2 \times 10^4$ and $3 \times 10^4$ CFU per organ 3 and 5 weeks

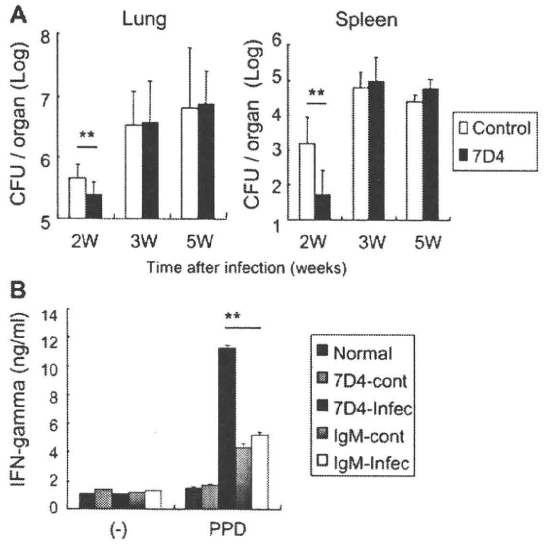


**Fig. 3.** The effect of CD25$^+$ cell depletion in *Mycobacterium tuberculosis* Erdman infection. (A) Control IgM-treated mice (open bars) and 7D4 anti-CD25 antibody-treated-mice (closed bars) were aerogenically infected with $5 \times 10^6$ CFU of *M. tuberculosis* Erdman. Bacterial numbers of lungs and spleens were measured at 2, 3 and 5 weeks post-infection. $^{**}P < 0.01$ versus control mice. (B) CD4$^+$ T cells from non-infected mice with 7D4 treatment (7D4-cont), *M. tuberculosis*-infected mice with 7D4 treatment (7D4-Infec), non-infected mice with control IgM treatment (IgM-cont) or *M. tuberculosis*-infected mice with control IgM treatment (IgM-Infec) were cultured with APC in the presence (PPD) or absence (−) of 10 μg ml$^{-1}$ PPD for 7 days. Production of IFN-gamma in the culture supernatants was analyzed. $^{**}P < 0.01$: *Mycobacterium tuberculosis*-infected mice with control IgM treatment (IgM-Infec) versus *M. tuberculosis*-infected mice with 7D4 treatment (7D4-Infec).

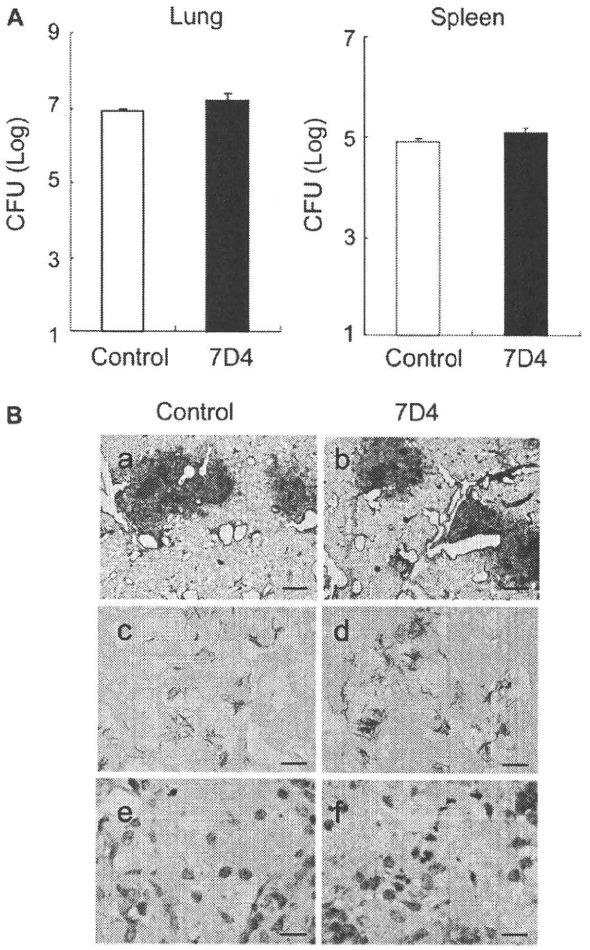


**Fig. 4.** The effect of depletion of CD25$^+$ cell in chronically infected mice with *M. tuberculosis*. DBA/2 mice were aerogenically infected with $5 \times 10^6$ CFU of *M. tuberculosis* H37Rv. Two months after infection, mice were treated with 1 mg of 7D4 or control IgM three times with 4 days interval. Five days later from final treatment, mice were sacrificed and analyzed. (A) Bacterial numbers in lungs (left panel) and spleens (right panel) of mice treated with control IgM (open bars) or 7D4 (closed bars). (B) Lung sections were stained with H&E (a and b), Ziehl–Neelsen (c and d) and Giemsa (e and f). Granulomas mainly consisted epithelioid macrophages (e and f). Numerous acid-fast bacteria were observed in granulomas of both control IgM- and 7D4-treated mice. (a, c and e) Lungs sections from mice treated with control IgM. (b, d and f) Lungs sections from mice treated with 7D4. Bars, 500 μm (a and b), 10 μm (c–f). Bars represent mean ±standard deviation of eight mice.

post-challenge, respectively (Fig. 2A). Depletion of CD25$^+$ cells resulted in significantly lower bacterial number in both lung and spleen 3 weeks after challenge; however, this effect became marginal 5 weeks post-challenge (Fig. 2A). Numerous bacteria were observed in granulomas of 7D4-treated and control mice after infection (Fig. 2B, e and f), consistent with higher bacterial burdens revealed by plating of organ homogenates (Fig. 2A). Histological examination of the lung correlated with the CFU results; 3 weeks post-infection, depletion of CD25$^+$ cells resulted in decreased granuloma formation compared with mice treated with control IgM, but normalized 5 weeks after challenge [Fig. 2B(a–d) and C]. Histopathology showed that granuloma cellular composition did not differ between 7D4-treated mice and control mice, which consisted predominately of epithelioid macrophages (Fig. 2B, g and h). Thus in *M. tuberculosis* Kurono infection, the effect of CD25$^+$ cell depletion was limited to the early phase of infection only.

To determine whether the transient effect of CD25$^+$ cells is specific for *M. tuberculosis* Kurono, we performed similar experiments employing another commonly used mycobacterial strain, *M. tuberculosis* Erdman. Similar results were observed in bacterial burdens: 7D4-treated mice revealed significantly lower bacterial numbers than those of IgM-treated mice at early stage (2 weeks post-infection), but not 3 weeks or 5 weeks post-challenge (Fig. 3A). Splenic CD4$^+$ T cells derived from 7D4-treated mice at this time point produced significantly higher levels of IFN-gamma than those of IgM-treated mice when stimulated with PPD (Fig. 3B).

We also examined the effects of depletion of CD25$^+$ cells on the survival of another mycobacterial strain, *Mycobacterium bovis* bacillus Calmette-Guérin (BCG). DBA/2 or BALB/c mice depleted of CD25$^+$ cells by 7D4 were challenged with BCG intravenously and the survival of BCG in the lungs

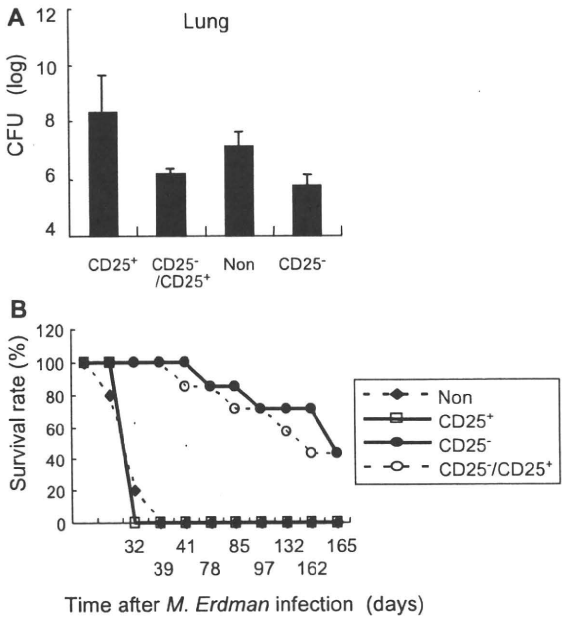


**Fig. 5.** Bacterial burden and survival kinetics of reconstituted SCID mice with T cell subsets after infection of *Mycobacterium tuberculosis* Erdman. (A) T cell subsets were isolated from spleens of chronically BCG-infected mice. SCID mice were reconstituted with $7.5\times10^5$ of $CD4^+CD25^+$ T cells only ($CD25^+$), $7.5\times10^5$ of $CD4^+CD25^-$ T cells and $7.5\times10^4$ of $CD4^+CD25^+$ T cells ($CD25^-/CD25^+$), untransferred (Non), and $7.5\times10^5$ of $CD4^+CD25^-$ T cells only ($CD25^-$). One day after reconstitution, naive or T cell subset-reconstituted SCID mice were aerogenically infected with $5\times10^6$ CFU *M. tuberculosis* Erdman. (B) Survival rates of naive or reconstituted SCID mice after infection. Time course of survival was examined up to 165 days post-infection. Five to eight mice per group were analyzed.

post-challenge was monitored. Unlike *M. tuberculosis*, there was no marked increase in BCG levels in the mouse lungs. Depletion of $CD25^+$ cells did not alter the survival ratio of BCG in the lungs of DBA/2 and BALB/c mice 3 and 5 weeks post-infection, although *in vitro* stimulation with PPD, lymphocytes derived from 7D4-treated mice at 3 weeks after challenge produced higher amount of IFN-gamma than those from control IgM-treated mice (data not shown).

*Depletion of $CD25^+$ cells in the chronic stage of infection does not affect the bacterial burdens and pathology*

We next examined the effects of depletion of $CD25^+$ cells in the late stage of mycobacterial infection. DBA/2 mice were airborne-infected with *M. tuberculosis* H37Rv and $CD25^+$ cells were depleted by 7D4 treatment after 60, 65 and 70 days later. Five days later from the final treatment of 7D4, we analyzed the bacterial burden and histology in the organs. Bacterial numbers of lungs and spleens in 7D4-treated mice were rather slightly higher than those in control IgM-treated mice; however, significant differences were not observed (Fig. 4A). Pulmonary granuloma formation was conspicuous in both 7D4-treated mice and control IgM-treated mice (Fig. 4B, a and b). Cellular composition of granuloma did not differ between 7D4-treated mice and control mice and numerous bacteria were observed in both groups of mice (Fig. 4B, c–f).

*$CD4^+CD25^+$ T cells do not suppress protection induced by $CD4^+CD25^-$ T cells against M. tuberculosis infection in reconstituted mice*

To further evaluate the role of $CD4^+CD25^+$ Treg cells in mycobacterial infection at late stage (after developing acquired immunity), the following experiment was conducted. $CD4^+CD25^-$ T cells and $CD4^+CD25^+$ T cells were purified from chronically BCG-infected mice: >90% of the $CD4^+CD25^+$ T cells obtained expressed FoxP3 as estimated by FACScan (data not shown). Each T cell subset, either alone or in combination, was then transferred into SCID mice and mice were infected with *M. tuberculosis* Erdman by airborne exposure. Three weeks post-infection, the bacterial number in lungs (Fig. 5A) and survival kinetics of mice (Fig. 5B) were analyzed.

Observed increases in *M. tuberculosis* were similar in both naive SCID mice and SCID mice reconstituted with $CD4^+CD25^+$ T cells alone, suggesting that $CD4^+CD25^+$ T cells offer no protection against *M. tuberculosis*. In contrast, SCID mice reconstituted with $CD4^+CD25^-$ T cells controlled *M. tuberculosis* infection, at a similar level to that of mice reconstituted with the combination of $CD4^+CD25^-$ T cells and $CD4^+CD25^+$ T cells (Fig. 5A). The survival kinetics showed similar outcomes between mice reconstituted with $CD4^+CD25^-$ T cells plus $CD4^+CD25^+$ T cells and $CD4^+CD25^-$ effector T cells alone (Fig. 5B). These data suggest that the role of $CD4^+CD25^+$ Treg cells in host protection is marginal against *M. tuberculosis* in the overall course of infection (Fig. 5B).

*Stimulation with mycobacterial antigens fails to express the function of $CD4^+CD25^+$ Treg cells in vitro*

To ascertain why $CD4^+CD25^+$ Treg cells have only a minor role in the late stage of mycobacterial infection, we compared the action of $CD4^+CD25^+$ T cells to $CD4^+CD25^-$ T cells *in vitro*. $CD4^+CD25^+$ and $CD4^+CD25^-$ T cells were isolated from normal mice or mice chronically infected with BCG or *M. tuberculosis* and stimulated with PPD or anti-CD3 mAb in the presence of APCs. $CD4^+CD25^+$ T cells alone showed characteristics of Treg cells, which neither proliferate nor produce cytokines in response to neither PPD nor anti-CD3 mAb (Fig. 6, A–J and a–e). Culture experiments using a combination of $CD4^+CD25^+$ and $CD4^+CD25^-$ T cells showed that $CD4^+CD25^+$ T cells derived from both normal and infected mice suppressed proliferation of $CD4^+CD25^-$ T cells and production of cytokines, such as IFN-gamma and IL-10, in a dose-dependent manner following stimulation with anti-CD3 mAb, showing the characteristics in Treg cells. However, following stimulation with PPD, $CD4^+CD25^+$ T cells failed to suppress both proliferation and production of cytokines. In contrast, IL-2 production was suppressed in a dose-dependent manner in the presence of PPD. Definitive IL-6 production was observed when $CD4^+CD25^-$ T cells were incubated alone or combination with $CD4^+CD25^+$ T cells in the presence of PPD (Fig. 6, I, J and e).

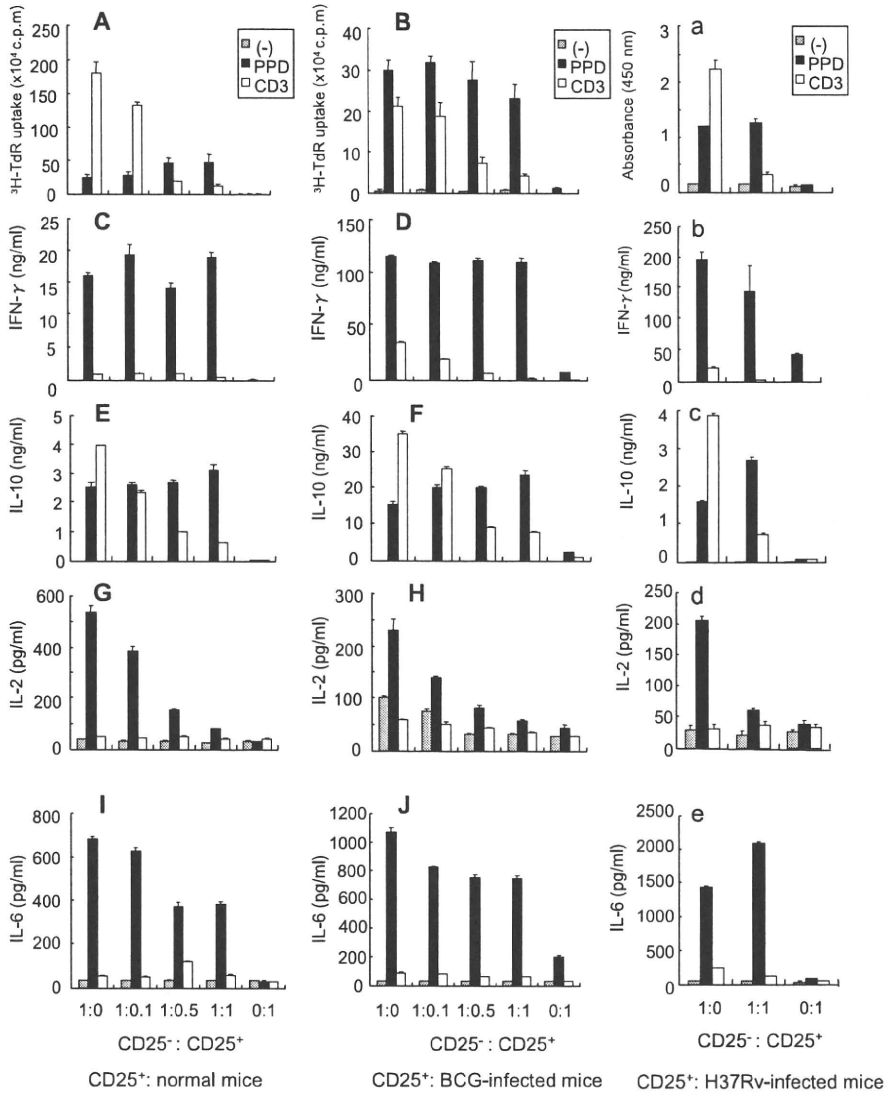


**Fig. 6.** Stimulation of CD4$^+$CD25$^+$ T cells by PPD fails to suppress the function of PPD-activated CD4$^+$CD25$^-$ T cells. CD4$^+$CD25$^+$ T cells (CD25$^+$) purified from normal (A, C, E, G and I) mice or mice chronically infected with BCG (B, D, F, H and J) or *Mycobacterium tuberculosis* (a–e) were co-cultured with CD4$^+$CD25$^-$ effector T cells (CD25$^-$) purified from mice chronically infected with BCG or *M. tuberculosis* at various ratios with T cell-depleted irradiated spleen cells (APCs) in the presence of PPD (PPD), or anti-CD3 mAb (CD3), or alone (–). Proliferative responses were analyzed at day 5 (A, B and a). Cytokine production in culture supernatants was measured at day 7 (C, E, I, J and b–e) or day 5 (D, F, G and H).

*Soluble mediators are not suppressive factors of CD4$^+$CD25$^+$ Treg cell function when stimulated with PPD*

Because IL-6 allows effector T cells to overcome suppression by CD4$^+$CD25$^+$ Treg cells (27), we considered the possibility that IL-6 inhibits the function of CD4$^+$CD25$^+$ Treg cells when stimulated with *M. tuberculosis*-derived mycobacterial antigen, PPD. Therefore, we neutralized IL-6 by neutralizing mAb; however, neutralization of IL-6 did not recover suppressive activity of CD4$^+$CD25$^+$ Treg cells (Fig. 7A and B).

To determine whether soluble factors beside IL-6 abrogate the suppressive function of CD4$^+$CD25$^+$ Treg cells upon PPD stimulation, we examined the effects of soluble factors released from T cells and APCs. The culture supernatants from CD4$^+$CD25$^+$ T cells cultured with both CD4$^+$CD25$^-$ T cells and APCs in the presence of PPD or anti-CD3 mAb were collected and then transferred to fresh culture of CD4$^+$CD25$^-$ T cells, CD4$^+$CD25$^+$ T cells and APCs in the presence or absence of anti-CD3 mAb. The proliferative response of CD4$^+$CD25$^-$ effector T cells was analyzed by incorporation of [$^3$H]TdR. The results showed that the supernatants of combined CD4$^+$CD25$^-$ and CD4$^+$CD25$^+$ T cell culture failed to diminish suppressive activity of proliferative response of CD4$^+$CD25$^-$ T cells by CD4$^+$CD25$^+$ T cell stimulated with anti-CD3 mAb (Fig. 8). These results show

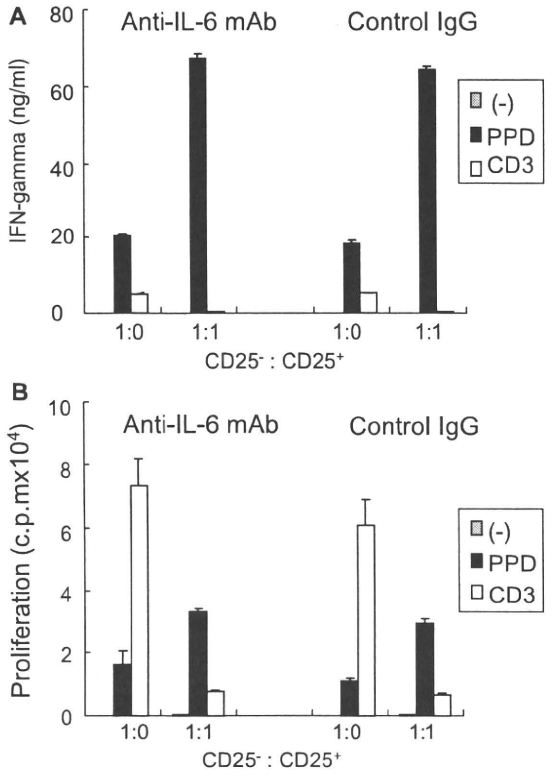


**Fig. 7.** Neutralization of IL-6 does not affect the $CD4^+CD25^+$ T cell-mediated suppression of the function of effector T cells. $CD4^+CD25^-$ T cells and $CD4^+CD25^+$ T cells were isolated from mice chronically infected with BCG. $CD4^+CD25^-$ effector T cells alone (1:0) or combination of $CD4^+CD25^-$ effector T cells and $CD4^+CD25^+$ T cells (1:1) were cultured with APCs in the presence of PPD (PPD), anti-CD3 mAb (CD3) or absence of these (−). In each well, 0.02 μg $ml^{-1}$ of anti-IL-6 mAb or control IgG were added. IFN-gamma production in culture supernatant (A) and proliferative responses of T cells (B) were analyzed at day 4.

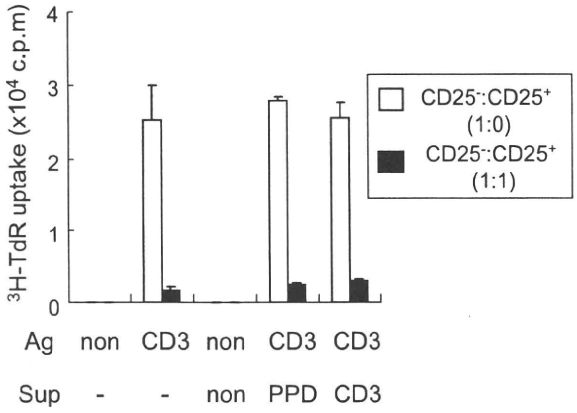


**Fig. 8.** Soluble mediators upon PPD stimulation do not abrogate $CD4^+CD25^+$ T cell-mediated suppression. $CD4^+CD25^-$ effector T cells ($CD25^-$) and $CD4^+CD25^+$ T cells ($CD25^+$) were isolated from spleens of chronically BCG-infected mice. $CD4^+CD25^-$ T cells/$CD4^+CD25^+$ T cells/APC (1:0:0.1) or $CD4^+CD25^-$ T cells/$CD4^+CD25^+$ cells/APC (1:1:0.1) were cultured with PPD (Sup, PPD), anti-CD3 mAb (Sup, CD3) or alone (Sup, non), for 7 days. Each culture supernatant was stored. Freshly isolated $CD4^+CD25^-$ T cells/$CD4^+CD25^+$ cells/APC (1:0:0.1) or $CD4^+CD25^-$ T cells/$CD4^+CD25^+$ cells/APC (1:1:0.1) were cultured 1:1stored supernatant: fresh culture medium in the presence (Ag, CD3) or absence (Ag, non) of anti-CD3 mAb. Proliferative responses were analyzed at day 4.

that the defective function of $CD4^+CD25^+$ Treg cells following PPD stimulation was not dependent on soluble factors released from T cells and APCs.

*Activated $CD4^+CD25^+$ Treg cells suppress the function of PPD-stimulated $CD4^+CD25^-$ effector T cells*

Two possibilities could explain the lack of effect of PPD-stimulated $CD4^+CD25^+$ Treg cells on the function of $CD4^+$ $CD25^-$ T cells. First, that activated $CD4^+CD25^+$ Treg cells fail to suppress the function of $CD4^+CD25^-$ T cells by mycobacterial antigens, and second that $CD4^+CD25^+$ Treg cells are not activated by mycobacterial antigens at the late stage of infection. To investigate these possibilities, we purified $CD4^+CD25^+$ T cells from chronically infected mice with BCG or *M. tuberculosis*, then activated *in vitro* with anti-CD3/CD28 mAb-coated beads in the presence of recombinant IL-2. The cells were then cultured with $CD4^+CD25^-$ T cells derived from BCG- or *M. tuberculosis*-infected mice in the presence of PPD. We found that activated $CD4^+CD25^+$ T cells unequivocally suppressed both proliferation and production of IFN-gamma of $CD4^+CD25^-$ T cells stimulated with PPD (Figs 9 and 10). Thus, our data show that both BCG and *M. tuberculosis* infection activate antigen-specific $CD4^+CD25^-$ effector T cells, but not $CD4^+CD25^+$ Treg cells, at the late stage of infection.

## Discussion

$CD4^+CD25^+$ Treg cells play a pivotal role in self-tolerance and autoimmune diseases and also in the progression of infectious diseases. It has been shown that $CD4^+CD25^+$ Treg cells are preventive against eradication of persistent pathogens, such as *Leishmania* protozoa, herpes simplex virus and HIV (17–20). Mycobacteria are major parasitic bacteria for eukaryotes (28). In this study, we investigated the role of $CD4^+CD25^+$ Treg cells in mycobacteria infection in mice.

We first studied the effects of Treg cell depletion against infection of mycobacteria. At the early stage of infection, depletion of $CD25^+$ cells significantly suppressed the growth of virulent *M. tuberculosis* strains, such as Kurono and Erdman, suggesting a role for $CD4^+CD25^+$ Treg cells in exacerbation of tuberculosis at the early stage of infection. This is consistent with the previous study performed by Kursar *et al.* (22). This effect of $CD4^+CD25^+$ Treg cells is presumably mediated through naturally occurring $CD4^+CD25^+$ Treg cells, which can be activated through Toll-like receptor (TLR)-mediated signaling (29–32). Mycobacterial DNA [TLR9 ligand (33)] and lipoproteins [TLR2 ligand (34)] may participate in activation of naturally occurring $CD4^+CD25^+$ Treg cells at this stage.

Two to three weeks post-infection, acquired immunity is evident (35). IFN-gamma producing T-helper 1 cells ($T_h1$) are major effectors in suppressing intracellular survival of

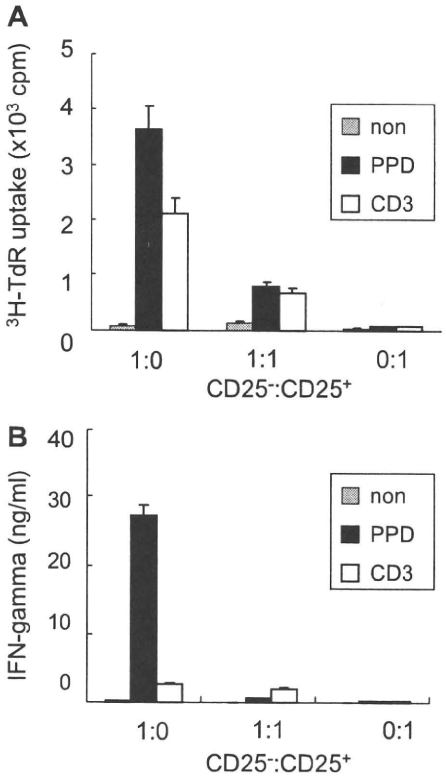


**Fig. 9.** *In vitro* activation of CD4$^+$CD25$^+$ T cells derived from BCG-infected mice inhibits the function of PPD-stimulated CD4$^+$CD25$^-$ effector T cells. CD4$^+$CD25$^+$ T cells obtained from chronically BCG-infected mice were activated by incubation with anti-CD3/CD28 mAb-coated beads at a bead:cell ratio 2:1 in the presence of 2000 U ml$^{-1}$ of recombinant mouse IL-2 for 48 h. Activated CD4$^+$CD25$^+$ T cells were co-cultured with freshly isolated CD4$^+$CD25$^-$ effector T cells in the presence of PPD (filled column), anti-CD3 mAb (open column) or alone (gray column). (A) Proliferation of CD4$^+$CD25$^-$ effector T cells wase analyzed at day 4. (B) IFN-gamma production in the culture supernatant as measured at day 7.

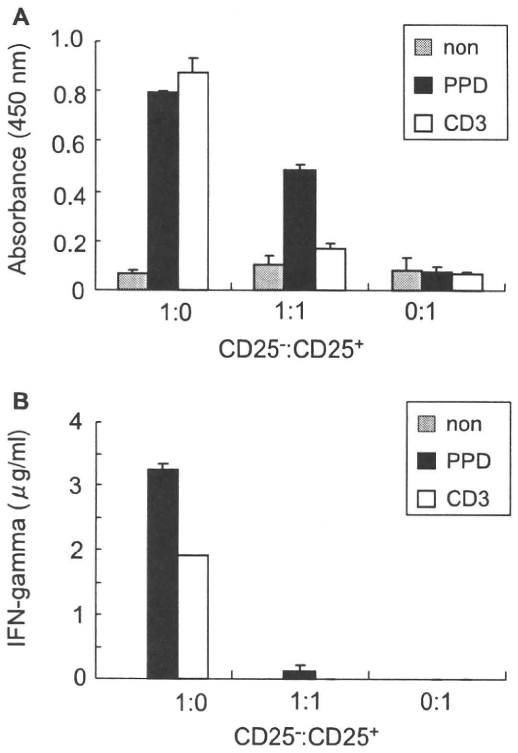


**Fig. 10.** *In vitro* activation of CD4$^+$CD25$^+$ T cells derived from *Mycobacterium tuberculosis*-infected mice inhibit the function of PPD-stimulated CD4$^+$CD25$^-$ effector T cells. CD4$^+$CD25$^+$ T cells obtained from chronically *M. tuberculosis* H37Rv-infected mice were activated by incubation with anti-CD3/CD28 mAb-coated beads at a bead:cell ratio of 2:1 in the presence of 2000 U ml$^{-1}$ of recombinant mouse IL-2 for 48 h. Activated CD4$^+$CD25$^+$ T cells were co-cultured with freshly isolated CD4$^+$CD25$^-$ effector T cells in the presence of PPD (filled column), anti-CD3 mAb (open column) or alone (gray column). (A) Proliferation of CD4$^+$CD25$^-$ effector T cells was analyzed at day 4. (B) IFN-gamma production in the culture supernatant as measured at day 7.

mycobacteria (36–38). In the CD25$^+$ cell-depletion experiments, the advantages of CD25$^+$ cell depletion were diminished 3 and 5 weeks after the challenge of *M. tuberculosis* Erdman and Kurono, respectively (Figs 2 and 3). We also found that persistence of BCG in mice is not altered by depletion of CD25$^+$ cells by 7D4 (data not shown). These data can be explained by the short-action profile of antibodies. However, we could not find any effect of depletion of CD25$^+$ cells at the chronic stage of infection (Fig. 4), when bacterial numbers were sustained at the same level (39). Similar results were obtained using another anti-CD25 mAb PC6C1, which causes significant reduction of the number of persistent *Leishmania major* in mice by suppressing CD4$^+$CD25$^+$ Treg cells (personal communication with Dr Alan Sher). Furthermore, our *in vivo* experiments in reconstituted SCID mice further suggest that the role of CD4$^+$CD25$^+$ Treg is minimal after infection is established (Fig. 5). The survival kinetics of mice reconstituted with CD4$^+$CD25$^-$ T cells alone are comparable to those in mice reconstituted with both CD4$^+$CD25$^-$ effector T cells and CD4$^+$CD25$^+$ Treg cells (10:1). These data indicate that CD4$^+$CD25$^+$ Treg cells have no impact on the overall outcome of *M. tuberculosis* infection. Kursar *et al.* suggested that CD4$^+$CD25$^+$ Treg cells prevent the bactericidal immune response based on data analyzed in RAG-KO mice reconstituted with each T cell subset (22). However, they reconstituted mice with T cells from naive animals at an unphysiological ratio of CD4$^+$CD25$^-$ T cells to CD4$^+$CD25$^+$ T cells (2:1). These differences may explain the discrepancy between studies.

In order to elucidate the cellular mechanisms of the minimal effect of CD4$^+$CD25$^+$ Treg cells in *M. tuberculosis* infection after the infection was established, we evaluated the function of CD4$^+$CD25$^+$ Treg cells *in vitro*. We activated each population of CD4$^+$ T cells derived from naive and BCG- or *M. tuberculosis*-chronically infected mice with anti-CD3 mAb or *M. tuberculosis*-derived antigens, PPD. BCG has >99.5% identical genome with that of *M. tuberculosis* (40) and therefore BCG and *M. tuberculosis* share almost identical antigens. CD4$^+$CD25$^+$ T cells suppressed anti-CD3-induced

activation (proliferation, production of IFN-gamma and IL-10) of $CD4^+CD25^-$ effector T cells whereas, reflecting our *in vivo* data, PPD stimulation failed to suppress the function of $CD4^+CD25^-$ effector T cells. Both $CD4^+CD25^-$ and $CD4^+CD25^+$ T cells consume IL-2 to proliferate or maintain the state but only $CD25^+CD25^-$ effector T cells produce IL-2. Thus, the level of IL-2 inversely correlated with the number of $CD4^+CD25^+$ T cells (Fig. 6G, H and d) is considered the results of consumption of IL-2 by $CD4^+CD25^+$ T cells but not functional suppression.

One of mechanisms of diminished Treg cell function is mediated by IL-6, which is produced by activated APC through TCR signaling (27). We observed obvious production of IL-6 with PPD stimulation, although which cells produced IL-6 was unknown (Fig. 6, I, J and e). However, neither IL-6 nor other soluble factors released from cells were involved in the non-functional property of $CD4^+CD25^+$ Treg cells following PPD stimulation (Fig. 8). An explanation for this phenomenon is that PPD-specific $CD4^+CD25^+$ Treg cells are not activated at the late stage of mycobacterial infection because $CD4^+CD25^+$ Treg cells activated by anti-CD3/CD28 suppress the function of $CD4^+CD25^-$ effector T cells following stimulation with PPD (Figs 9 and 10).

With the exception of one recent study on herpes simplex virus infection (41), $CD4^+CD25^+$ Treg cells are thought to support parasite persistence in the host by inhibiting the function of effector T cells by a variety of mechanisms. According to this theory, several reports regarding mycobacterial infection have suggested a role for $CD4^+CD25^+$ Treg cells in disease progression and establishment of latent infection (22, 25, 42). However, our findings refute this theory, because $CD4^+CD25^+$ cells did not affect the total infectious load of *M. tuberculosis* in mice (Fig. 5) and mycobacterial infection did not activate mycobacteria-specific $CD4^+CD25^+$ Treg cells (Figs 6, 9 and 10). Several reports showed that FoxP3-positive Treg cells are found in the site of infection with BCG or *M. tuberculosis* (23, 25, 42). However, we consider that these Treg cells are unresponsive to mycobacterial antigens, rather than responding to self-antigens in the disrupted tissues of the infectious legion (43).

In contrast, $CD4^+CD25^+$ Treg cells responding to parasite antigens are activated during infection of *Leishmania* (17, 44) and *Plasmodium* (21). These parasites more closely resemble mammals in the history of evolution; therefore, it can be speculated that they express antigens similar to mammalian self-antigens, which leads to activation of self-antigen-reactive $CD4^+CD25^+$ Treg cells (43). This may be a possible reason for the discrepancy of the host response to mycobacteria versus protozoa. The host must recognize pathogens to survive and mycobacteria represent major bacterial pathogens for vertebrates. In our study, the fact that effector T cells are activated in response to mycobacterial antigens, while suppressive $CD4^+CD25^+$ Treg cells are comparatively silent, is rational based on the host's need to protect itself from mycobacterial infection.

## Funding

Japan Health Sciences Foundation; Ministry of Health, Labour and Welfare (Research on Emerging and Re-emerging Infectious Diseases, Health Sciences Research Grants); Ministry of Education, Culture, Sports, Science and Technology; Osaka City University Urban Research; Biochemical Tokyo Research Foundation, and The United States-Japan Cooperative Medical Science Program Against Tuberculosis Leprosy.

## Acknowledgements

We would like to thank Dr Toshiki Tamura and Dr Hidefumi Kojima for their advice and Mr Satoru Iwatani for technical support of FACS analysis. We also thank Dr Saburo Yamamoto and Miss Sara Matsumoto for heartfelt encouragement. The authors have no conflicting financial interests.

## References

1 Dye, C., Scheele, S., Dolin, P., Pathania, V. and Raviglione, M. C. 1999. Consensus statement. Global burden of tuberculosis: estimated incidence, prevalence, and mortality by country. WHO Global Surveillance and Monitoring Project. *JAMA* 282:677.
2 Jouanguy, E., Altare, F., Lamhamedi, S. *et al.* 1996. Interferon-gamma-receptor deficiency in an infant with fatal bacille Calmette-Guerin infection. *N. Engl. J. Med.* 335:1956.
3 Newport, M. J., Huxley, C. M., Huston, S. *et al.* 1996. A mutation in the interferon-gamma-receptor gene and susceptibility to mycobacterial infection. *N. Engl. J. Med.* 335:1941.
4 Sakaguchi, S. 2000. Regulatory T cells: key controllers of immunologic self-tolerance. *Cell* 101:455.
5 Sakaguchi, S. 2004. Naturally arising CD4+ regulatory t cells for immunologic self-tolerance and negative control of immune responses. *Annu. Rev. Immunol.* 22:531.
6 Shevach, E. M. 2001. Certified professionals: CD4(+)CD25(+) suppressor T cells. *J. Exp. Med.* 193:F41.
7 Read, S., Malmstrom, V. and Powrie, F. 2000. Cytotoxic T lymphocyte-associated antigen 4 plays an essential role in the function of CD25(+)CD4(+) regulatory cells that control intestinal inflammation. *J. Exp. Med.* 192:295.
8 Takahashi, T., Tagami, T., Yamazaki, S. *et al.* 2000. Immunologic self-tolerance maintained by CD25(+)CD4(+) regulatory T cells constitutively expressing cytotoxic T lymphocyte-associated antigen 4. *J. Exp. Med.* 192:303.
9 Shimizu, J., Yamazaki, S., Takahashi, T., Ishida, Y. and Sakaguchi, S. 2002. Stimulation of CD25(+)CD4(+) regulatory T cells through GITR breaks immunological self-tolerance. *Nat. Immunol.* 3:135.
10 McHugh, R. S., Whitters, M. J., Piccirillo, C. A. *et al.* 2002. CD4(+)CD25(+) immunoregulatory T cells: gene expression analysis reveals a functional role for the glucocorticoid-induced TNF receptor. *Immunity* 16:311.
11 Hori, S., Nomura, T. and Sakaguchi, S. 2003. Control of regulatory T cell development by the transcription factor Foxp3. *Science* 299:1057.
12 Sakaguchi, S., Yamaguchi, T., Nomura, T. and Ono, M. 2008. Regulatory T cells and immune tolerance. *Cell* 133:775.
13 Asseman, C., Mauze, S., Leach, M. W., Coffman, R. L. and Powrie, F. 1999. An essential role for interleukin 10 in the function of regulatory T cells that inhibit intestinal inflammation. *J. Exp. Med.* 190:995.
14 Gorelik, L. and Flavell, R. A. 2000. Abrogation of TGFbeta signaling in T cells leads to spontaneous T cell differentiation and autoimmune disease. *Immunity* 12:171.
15 Takahashi, T., Kuniyasu, Y., Toda, M. *et al.* 1998. Immunologic self-tolerance maintained by CD25+CD4+ naturally anergic and suppressive T cells: induction of autoimmune disease by breaking their anergic/suppressive state. *Int. Immunol.* 10:1969.
16 Thornton, A. M. and Shevach, E. M. 1998. CD4+CD25+ immunoregulatory T cells suppress polyclonal T cell activation *in vitro* by inhibiting interleukin 2 production. *J. Exp. Med.* 188:287.
17 Belkaid, Y., Piccirillo, C. A., Mendez, S., Shevach, E. M. and Sacks, D. L. 2002. CD4+CD25+ regulatory T cells control Leishmania major persistence and immunity. *Nature* 420:502.
18 Suvas, S., Kumaraguru, U., Pack, C. D., Lee, S. and Rouse, B. T. 2003. CD4+CD25+ T cells regulate virus-specific primary and memory CD8+ T cell responses. *J. Exp. Med.* 198:889.

19 Aandahl, E. M., Michaelsson, J., Moretto, W. J., Hecht, F. M. and Nixon, D. F. 2004. Human CD4+ CD25+ regulatory T cells control T-cell responses to human immunodeficiency virus and cytomegalovirus antigens. *J. Virol.* 78:2454.

20 Lundgren, A., Suri-Payer, E., Enarsson, K. *et al.* 2003. Helicobacter pylori-specific $CD4^+$ CD25high regulatory T cells suppress memory T-cell responses to H. pylori in infected individuals CD4 T cell activation by myelin oligodendrocyte glycoprotein is suppressed by adult but not cord blood $CD25^+$ T cells. *Infect. Immun.* 71:1755.

21 Hisaeda, H., Maekawa, Y., Iwakawa, D. *et al.* 2004. Escape of malaria parasites from host immunity requires $CD4^+$ $CD25^+$ regulatory T cells. *Nat. Med.* 10:29.

22 Kursar, M., Koch, M., Mittrucker, H. W. *et al.* 2007. Cutting Edge: regulatory T cells prevent efficient clearance of Mycobacterium tuberculosis. *J. Immunol.* 178:2661.

23 Quinn, K. M., McHugh, R. S., Rich, F. J. *et al.* 2006. Inactivation of CD4+ CD25+ regulatory T cells during early mycobacterial infection increases cytokine production but does not affect pathogen load. *Immunol. Cell Biol.* 84:467.

24 Quinn, K. M., Rich, F. J., Goldsack, L. M. *et al.* 2008. Accelerating the secondary immune response by inactivating CD4(+)CD25(+) T regulatory cells prior to BCG vaccination does not enhance protection against tuberculosis. *Eur. J. Immunol.* 38:695.

25 Scott-Browne, J. P., Shafiani, S., Tucker-Heard, G. *et al.* 2007. Expansion and function of Foxp3-expressing T regulatory cells during tuberculosis. *J. Exp. Med.* 204:2159.

26 Kaneko, H., Yamada, H., Mizuno, S. *et al.* 1999. Role of tumor necrosis factor-alpha in *Mycobacterium*-induced granuloma formation in tumor necrosis factor-alpha-deficient mice. *Lab. Invest.* 79:379.

27 Pasare, C. and Medzhitov, R. 2003. Toll pathway-dependent blockade of CD4+CD25+ T cell-mediated suppression by dendritic cells. *Science* 299:1033.

28 Flynn, J. L. and Chan, J. 2001. Immunology of tuberculosis. *Annu. Rev. Immunol.* 19:93.

29 Caramalho, I., Lopes-Carvalho, T., Ostler, D., Zelenay, S., Haury, M. and Demengeot, J. 2003. Regulatory T cells selectively express toll-like receptors and are activated by lipopolysaccharide. *J. Exp. Med.* 197:403.

30 Crellin, N. K., Garcia, R. V., Hadisfar, O., Allan, S. E., Steiner, T. S. and Levings, M. K. 2005. Human CD4+ T cells express TLR5 and its ligand flagellin enhances the suppressive capacity and expression of FOXP3 in CD4+CD25+ T regulatory cells. *J. Immunol.* 175:8051.

31 Peng, G., Guo, Z., Kiniwa, Y. *et al.* 2005. Toll-like receptor 8-mediated reversal of CD4+ regulatory T cell function. *Science* 309:1380.

32 Sutmuller, R. P., den Brok, M. H., Kramer, M. *et al.* 2006. Toll-like receptor 2 controls expansion and function of regulatory T cells. *J. Clin. Invest.* 116:485.

33 Bafica, A., Scanga, C. A., Feng, C. G., Leifer, C., Cheever, A. and Sher, A. 2005. TLR9 regulates Th1 responses and cooperates with TLR2 in mediating optimal resistance to *Mycobacterium tuberculosis*. *J. Exp. Med.* 202:1715.

34 Thoma-Uszynski, S., Stenger, S., Takeuchi, O. *et al.* 2001. Induction of direct antimicrobial activity through mammalian toll-like receptors. *Science* 291:1544.

35 North, R. J. and Jung, Y. J. 2004. Immunity to tuberculosis. *Annu. Rev. Immunol.* 22:599.

36 Flynn, J. L., Chan, J., Triebold, K. J., Dalton, D. K., Stewart, T. A. and Bloom, B. R. 1993. An essential role for interferon gamma in resistance to *Mycobacterium tuberculosis* infection. *J. Exp. Med.* 178:2249.

37 Cooper, A. M., Dalton, D. K., Stewart, T. A., Griffin, J. P., Russell, D. G. and Orme, I. M. 1993. Disseminated tuberculosis in interferon gamma gene-disrupted mice. *J. Exp. Med.* 178:2243.

38 Scanga, C. A., Mohan, V. P., Yu, K. *et al.* 2000. Depletion of CD4(+) T cells causes reactivation of murine persistent tuberculosis despite continued expression of interferon gamma and nitric oxide synthase 2. *J. Exp. Med.* 192:347.

39 Jung, Y. J., LaCourse, R., Ryan, L. and North, R. J. 2002. Evidence inconsistent with a negative influence of T helper 2 cells on protection afforded by a dominant T helper 1 response against Mycobacterium tuberculosis lung infection in mice. *Infect. Immun.* 70:6436.

40 Behr, M. A., Wilson, M. A., Gill, W. P. *et al.* 1999. Comparative genomics of BCG vaccines by whole-genome DNA microarray. *Science* 284:1520.

41 Lund, J. M., Hsing, L., Pham, T. T. and Rudensky, A. Y. 2008. Coordination of early protective immunity to viral infection by regulatory T cells. *Science* 320:1220.

42 Roberts, T., Beyers, N., Aguirre, A. and Walzl, G. 2007. Immunosuppression during active tuberculosis is characterized by decreased interferon- gamma production and CD25 expression with elevated forkhead box P3, transforming growth factor-beta, and interleukin-4 mRNA levels. *J. Infect. Dis.* 195:870.

43 Nishikawa, H., Kato, T., Tawara, I. *et al.* 2005. Definition of target antigens for naturally occurring CD4(+) CD25(+) regulatory T cells. *J. Exp. Med.* 201:681.

44 Mendez, S., Reckling, S. K., Piccirillo, C. A., Sacks, D. and Belkaid, Y. 2004. Role for CD4(+) CD25(+) regulatory T cells in reactivation of persistent leishmaniasis and control of concomitant immunity. *J. Exp. Med.* 200:201.

Jalilian *et al. Genetic Vaccines and Therapy* 2010, **8**:4
http://www.gvt-journal.com/content/8/1/4

GENETIC VACCINES AND THERAPY

RESEARCH Open Access

# Development of avian influenza virus H5 DNA vaccine and MDP-1 gene of *Mycobacterium bovis* as genetic adjuvant

Babak Jalilian[1], Abdul Rahman Omar*[1,2], Mohd Hair Bejo[2], Noorjahan Banu Alitheen[3], Mehdi Rasoli[1] and Sohkichi Matsumoto[4]

**Abstract**

**Background:** Studies have shown that DNA vaccines can induce protective immunity, which demonstrated the high potential of DNA vaccines as an alternative to inactivated vaccines. Vaccines are frequently formulated with adjuvants to improve their release, delivery and presentation to the host immune system.

**Methods:** The H5 gene of H5N1 virus (A/Ck/Malaysia/5858/04) was cloned separately into pcDNA3.1 + vector. The immunogenicity of the cloned H5 DNA vaccine was tested on SPF chickens using two different approaches. First approach was using H5 DNA vaccine (pcDNA3.1/H5) and the second was using H5 DNA vaccine in addition to the pcDNA3.1/MDP1 vaccine. Ten days old chickens inoculated three times with two weeks intervals. The spleen and muscle samples from chickens immunized with H5 (pcDNA3.1/H5) and H5 + MDP1 (pcDNA3.1/H5 + pcDNA3.1/MDP1) vaccines were collected after sacrificing the chickens and successfully expressed H5 and MDP1 RNA transcripts. The sera of immunized chickens were collected prior to first immunization and every week after immunization; and analyzed using enzyme-linked immunosorbent assay (ELISA) and hemagglutination inhibition (HI) test.

**Results:** Results of competitive ELISA showed successful antibody responses two weeks post immunization. The HI test showed an increased in antibody titers during the course of experiment in group immunized with H5 and H5 + MDP1 vaccines. The result showed that the constructed DNA vaccines were able to produce detectable antibody titer in which the group immunized with H5 + MDP1 vaccine produced higher antibody comparing to H5 vaccine alone.

**Conclusions:** This study shows for the first time the usefulness of MDP1 as a genetic adjuvant for H5 DNA vaccine.

## Background

Influenza virus can cause an acute, highly transmittable respiratory disease, which can result in high morbidity and mortality in both human and animals [1]. The 1997 Hong Kong outbreak of highly pathogenic avian influenza virus (HPAI)-H5N1 showed that avian influenza is a potential threat to human and is believed to be transmitted from infected birds [2]. The Hong Kong outbreak of avian influenza H5N1 was controlled by slaughtering 1.5 million chickens, which cost more than 245 million dollars in a single month. Therefore, antivirals and vaccines seem to be a more prospective solution to control the outbreaks of avian influenza virus [2].

Currently, whole virus inactivated vaccines containing HA as the main component, are the common vaccines to prevent avian influenza. However, these vaccines require large numbers of specific-pathogen-free embryonated chicken eggs and about 6 months to propagate the viruses [2]. On the other hand, this is not an ideal method to produce inactivated vaccine for highly pathogenic strains, as the embryos are killed shortly after propagation and require a high level of biosecurity to handle [3]. Commercial vaccines have been successful in producing protective immunity against infections by homologous virus but failed in preventing the outbreaks of heterologous virus and occasionally been reported as a possible cause of re-emerging outbreaks [2]. The commercially available vac-

* Correspondence: aro@ibs.upm.edu.my
[1] Institute of Bioscience, University Putra Malaysia, Serdang 43400, Selangor, Malaysia
Full list of author information is available at the end of the article

cines against H5N1 are inactivated whole virus vaccine and fowlpox virus vaccine expressing the H5 gene [4]. Moreover, various recombinant vaccines against avian influenza H5N1 virus which are able to induce different levels of protective immunity, such as DNA plasmid-based vaccine, baculovirus recombinant H5 vaccine, and reverse genetic H5 vaccine have been examined experimentally [5-7].

Concurrent studies have revealed that DNA vaccines encoding HA of influenza A virus can result in the development of protective immune response against influenza virus challenge in animals [8,9]. In most cases, two or three doses of naked plasmid DNA are required to induce immune response to the pathogen [10,11]. Nevertheless, other studies have shown that a single dose of DNA vaccine can trigger protective immunity, which demonstrated the high potential of DNA vaccines as an alternative to inactivated vaccines [12,13]. Recently, we have showed that the fusion of ESAT-6 of *Mycobacterium tuberculosis* to H5 DNA vaccine are able to improve the antibody titer of chickens against AIV showing the flexibility of modifying the efficacy of DNA vaccine [14].

Mycobacterial DNA binding protein 1 (MDP1) is a main cellular protein produced by *Mycobacterium bovis*. The protein has both nucleic acid binding activity and macro-molecular bio-synthesis inhibitory properties that play key role in modulating bacterial growth [15]. Prabhakar *et al.*, in 1998, revealed that DNA binding proteins (orthologus with MDP1) may act as an immunodominant antigen which stimulates cellular and humoral responses presumably through TLR9 dependent pathway production of proinflammatory cytokines [16,17] and the induction of IFN-γ production [18,19].

Hence, MDP1 may play an important role as a potential adjuvant to boost the immunotherapeutic effects of DNA vaccines.

## Methods

### Construction of recombinant DNA plasmids

Construction of eukaryotic expression plasmids were performed by separately cloning the HA gene of H5N1 AIV (A/chicken/H5N1/5858/2004) and MDP1 gene of *Mycobacterium bovis* into pcDNA3.1 + vectors (Invitrogen®, USA). The full length H5 gene (1707 bp) was amplified from pCR2.1/H5 (kindly provided by Nurul Hidayah, Biologics Lab, University Putra Malaysia) using forward and reverse primers with *Hind*III and *Bam*HI sites, respectively (Table 1). The MDP1 gene which was provided by Prof. Dr. Sohkichi Matsumoto from Department of Bacteriology, Osaka City University Graduate School of Medicine, Osaka, Japan; was amplified from pcDNA3.1/MDP1 using forward and reverse primers with *Hind*III and *Bam*HI sites, respectively (Table 1). The amplified genes of H5 and MDP1 were digested with *Hin-dIII* and *Bam*HI to generate cohesive ends for cloning into pcDNA3.1. The digested products were purified by electrophoresis and ligated into pcDNA3.1 using T4 ligation system (Vivantis®, Malaysia). The constructed plasmids were transformed into competent *Escherichia coli* Top10F' and cultured overnight for further application.

A PCR screening approach was used to detect the presence of the desired ligated DNA on the recombinant plasmids using the same forward and reverse primers which were used in amplifying H5 and MDP1 genes, respectively (Table 1). The selected recombinant clones were further confirmed by restriction enzyme (RE) analysis and sequencing. Sequencing was carried out using a 48 capillary 3730 DNA Analyzer® (Applied Biosystems®, USA) with both the aforementioned primers for H5 and MDP1 genes as well as the T7 promoter and BGH reverse universal primers.

### Transfection

Cell culture technology was used to test the *in vitro* expression of the genes of interest from the cloned plasmid. Vero cells (passage 71) were maintained in DMEM media (Gibco®, England) containing 10% bovine fetal serum (BFS) (HyClone®) and 1% ampicillin (50 μg/ml) (Biobasic Inc. ®). The day before transfection, cells were sub-cultured in a 6-well plate to have 80% confluency on the day of transfection. Transfection of each plasmid was performed using Lipofectamine™ 2000 according to the manufacturer's protocol in which 100 μl of Opti-MEM® was mixed with 1 μg of desired plasmid. The plate was incubated and the cells were harvested at 24, 48 and 72 hours post transfection for the detection of protein expression using SDS-PAGE and Western blotting assays.

### Western blotting

Prior to Western blotting, a SDS-PAGE gel was run using a BenchMark™ pre-stained protein ladder (Invitrogen®, USA). A BioRad® transblot machine was then used to transfer the expressed proteins from the SDS-PAGE gel to a nitrocellulose membrane using a constant current of 15 volt and 60 mA for 90 minutes. To detect the expression of different proteins, the membrane was incubated with different primary antibodies. Detection of H5 protein were performed using rabbit polyclonal antibody against AIV hemagglutinin A/chicken/Jilin/9/2004 (H5N1) (diluted 1:4000) (AbCam®, USA), whilst expression of MDP1 with MDP1 monoclonal antibody (1:200) which was provided by Prof. Dr. Sohkichi Matsumoto. The membranes were incubated with primary antibody solution for 1.5 hours at room temperature. The membrane was then incubated in anti-rabbit secondary antibody solution (diluted 1:4000) (AbCam®, USA), for 45 minutes at room temperature on a rotary shaker. Finally, the membrane was incubated in 5 ml of chromogenic

**Table 1: Primers designed for amplification of H5 and MDP1 genes.**

| Name | Type | Sequence (5' to 3') |
|---|---|---|
| H5 | F | CCC CAA GCT TAT GGA GAA AAT AGT GCT T |
| | R | CCC GGA TCC AAT GCA AAT TCT GCA TTG TAA |
| MDP1 | F | CCC AAG CTT ATG AAC AAA GCA GAG CTC |
| | R | AAA GGA TCC CTA TTT GCG ACC CCG |

F: Forward, R: Reverse
Underlined sequences are the restriction enzyme sites

solution (BCIP/NBT substrate for alkaline phosphatase) until the bands appeared.

### Immunization of the chickens with constructed DNA vaccines

Briefly, agar plate containing 50 μg/ml ampicillin was cultured using the glycerol stock of target plasmid overnight at 37°C. A single colony from the plate was cultured in 5 ml of LB broth containing 50 μg/ml ampicillin at 37°C for 8 hours with vigorous shaking. Two ml of the culture was inoculated in 200 ml of LB broth with 50 μg/ml ampicillin and shaked vigorously at 37°C for 15 hours. The bacterial pellet was obtained by centrifuging the culture in 200 ml centrifuge tubes at 6000 × g for 15 minutes at 4°C. The plasmids were then extracted using EndoFree®Plasmid Mega Kit (Qiagen®, Germany). The concentration and purity of the plasmid were determined using BioRad smart spec™ 3000 spectrophotometer. The solution was adjusted to 1 μg/μl and stored at -30°C for immunization trials. Specific-pathogen-free white Leghorn layer chickens were kept in separate cages for each group and fed twice a day using commercial chicken pellet while water was provided ad libitum. Ten days old chickens were tagged using metal wing tags and divided into five different groups with nine chickens in each group, namely H5, H5 + MDP1, pcDNA3.1 +, PBS and control. The last three groups were the different categories of negative control groups consisting of chickens immunized with parental plasmid alone, saline and left unimmunized, respectively. Ten days old chickens were immunized with 100 μg of purified plasmid via intramuscular route on the right pectoral muscle. The chickens in H5 + MDP1 group were immunized with 100 μg of H5 vaccine on the right and 100 μg of MDP1 vaccine on the left pectoral muscles. Two booster immunizations were administered within two weeks intervals after the first immunization. The first bleeding was performed via wing vein prior to the first vaccination and repeated every week post immunization for 5 weeks. The immunization trials followed internationally recognized guidelines and approved by animal care and use committee (Ref No. UPM/FPV/PS/3.2.1.551/AUP-R51) at the Faculty of Veterinary Medicine, University Putra Malaysia.

### Enzyme-linked immunosorbent assay (ELISA)

The sera derived from immunized and control chickens were subjected to a competitive ELISA test using a qualitative ELISA kit (AniGene®, Korea). Briefly, the plates were pre-coated with recombinant H5 avian influenza virus antigen (Anigen® H5 AIV Ag). Fifty μl of serum and 50 μl of Mab-HRP were added to the wells and incubated for 90 minutes at 37°C. The wells were then aspirated and washed several times to remove the unbounded material. Following that the substrate solution was added to the wells and incubated at room temperature for one hour. The reaction was stopped by adding the stop solution and a spectrophotometer (450 nm and 620 nm) were used to read the colorimetric results. The percent inhibition (PI) value was calculated using, PI value = [1 - (OD sample/mean OD negative)] × 100 formula in which the samples with PI value of 50 and more were considered positive.

### Hemagglutination inhibition assay (HI)

The HI test was performed using the serum samples obtained from chickens immunized with different DNA vaccines. A low pathogenic H5 AIV, [A/MY/Duck/8443/04 (H5N2)] inactivated in 2-bromoethylenne hydrobromide, titrated at 4 HA/25 μl were used in the test. Briefly, 50 μl of serum was added to the first well and serially diluted to the 11$^{th}$ well (1:2 to 1:1024). The diluted serum was then incubated with 25 μl of inactivated H5N2 virus at room temperature for 20 minutes. Twenty five μl of 0.65% washed chicken RBC was added to all the wells in plate and incubated for 30 minutes. The test results were read on a plate reader apparatus and statistically analyzed using repeated measure ANOVA. The sequence analysis of the H5 of the H5N2 showed more than 87% similar with the H5 of H5N1 in use (data not shown).

### Reverse transcription-polymerase chain reaction

The chickens were sacrificed one week after second booster. The spleen and muscle samples from the injection site were harvested and used for RT-PCR. Total RNA extraction of the samples was performed using Trizol® as described by the manufacturer (Tri Reagent®, Life Technologies, USA). The extracted RNA was subjected to RT-PCR using a commercial RT-PCR kit (Promega®, USA). The PCR mixture and condition were carried out as described previously by Oveissi *et al.* with slight modifications [14]. The extracted RNA was subjected to RT-PCR using a commercial RT-PCR kit (Promega®, USA). AMV Reverse Transcriptase High Conc. (15 units/mg) was used to reverse transcribe 2 μg of respective RNA in the presence of dNTP's (250 mM), reverse transcriptase buffer (10 mMTris-HCl, 50 mMKCl, 0.1% TritonR-X-100), oligo dT primers (0.5 mg) and RNasin Ribonuclease inhibitor (1 unit/ml). The amplified product was run in 2.5% agarose gel at 70 volt for 45 minutes. The RNA preparations were standardized by RT-PCR for β-Actin and were free from DNA contamination evaluated by the lack of signal following non-reverse transcribed RNA using the same samples and set of primers (Table 2).

## Results

### Cloning of the H5 and MDP1 gene into the pcDNA3.1 + vector

The constructed pcDNA3.1/H5 and pcDNA3.1/MDP1 were transformed into TOP10F' *Escherichia coli* and the positive clones were screened using PCR, RE analysis and sequencing. Digestion with *Bam*HI and *Hind*III confirmed the presence of H5 and MDP1 based on the detection of the bands of the expected sizes (data not shown). The sequencing results were checked with the original sequence of the genes deposited in the GeneBank database using the Blast program of National Institute of Biotechnology Information (NCBI).

### Transient expression of the recombinant plasmids in Vero cells

The expressions of H5 and MDP1 genes in Vero cells were analyzed by SDS-PAGE and Western blot. In Western blot analysis, expressed proteins for H5 (64 kDa) (Figure 1A) were detected 72 hours after transfection while the expressed protein for MDP1 (31 kDa) (Figure 1B) were successfully detected 48 and 72 hours after transfection.

### Enzyme-linked immunosorbent assay

The AIV H5 antibody was successfully detected by a competitive ELISA starting at 21 days post immunization on two out of nine chickens immunized with H5 + MDP1 vaccine. At 42 days post immunization eight out of nine chickens in the above group demonstrated antibody responses against AIV (Table 3). However, the number of chickens with antibody responses in group immunized with H5 alone is lower compared to chickens immunized with H5 + MDP1. Only five out of nine chickens in the H5 group demonstrated antibody responses at day 42 post immunization, as shown in Table 3. Chickens from the negative control groups (pcDNA3.1/MDP1, pcDNA3.1 and left unimmunized) failed to demonstrate detectable antibody response (Table 3).

### Hemagglutination inhibition assay

The HI titer of the serum samples two weeks after the first vaccination was zero or very low (≤ 2). All the chickens in the group immunized with H5 vaccine and H5 + MDP1 vaccines showed HI antibody titer at day 21 post immunization (Table 4). The chickens in group immunized with H5 + MDP1 vaccines have slightly higher mean HI titer (3.33 ± 2.42) compared to chickens in the group immunized with H5 vaccine alone (2.33 ± 0.82). The increase in the HI titers was recorded in both groups at two weeks after the first booster and one week after the second booster. The mean HI titers from chickens immu-

**Table 2: Primers for RT-PCR amplification of H5, MDP1 and β actin genes**

| Name | Type | Sequence (5' to 3') | Length (bp) | Product |
|---|---|---|---|---|
| H5 | F | TCCAAAGTAAACGGGCAAAG | 20 | 141 bp |
| | R | TGYTGAGTCCCCTTTCTTGA | 20 | |
| MDP1 | F | TCACACAGAAATTGGGCTCGGA | 22 | 196 bp |
| | R | GACGTCGGCTTCACCTTTACTG | 22 | |
| β actin | F | GCAGGAGTACGATGAATC | 18 | 140 bp |
| | R | AAATAAAGCCATGCCAATC | 19 | |

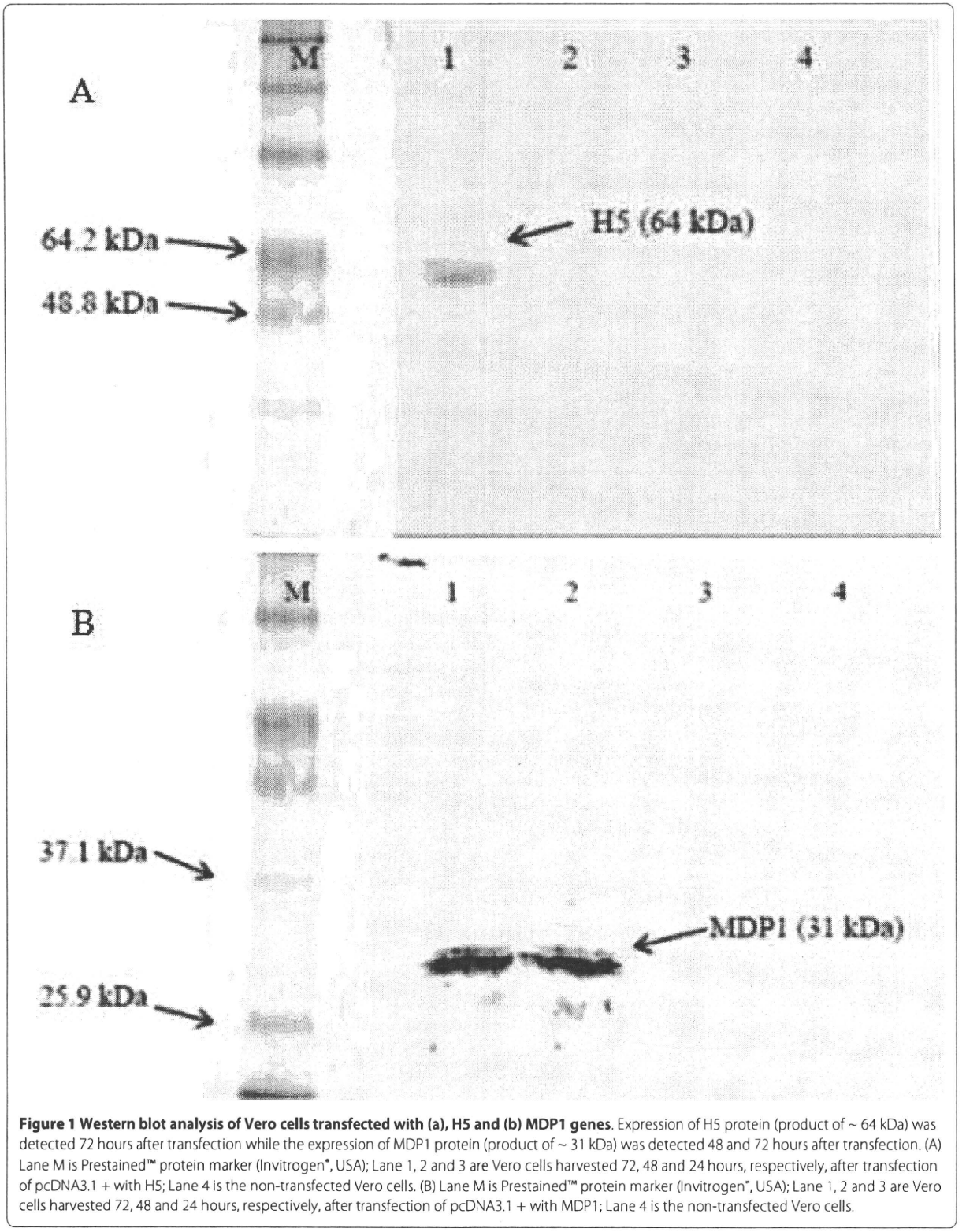


**Figure 1 Western blot analysis of Vero cells transfected with (a), H5 and (b) MDP1 genes**. Expression of H5 protein (product of ~ 64 kDa) was detected 72 hours after transfection while the expression of MDP1 protein (product of ~ 31 kDa) was detected 48 and 72 hours after transfection. (A) Lane M is Prestained™ protein marker (Invitrogen®, USA); Lane 1, 2 and 3 are Vero cells harvested 72, 48 and 24 hours, respectively, after transfection of pcDNA3.1 + with H5; Lane 4 is the non-transfected Vero cells. (B) Lane M is Prestained™ protein marker (Invitrogen®, USA); Lane 1, 2 and 3 are Vero cells harvested 72, 48 and 24 hours, respectively, after transfection of pcDNA3.1 + with MDP1; Lane 4 is the non-transfected Vero cells.

**Table 3: Detection of H5 AIV antibody from serum samples using ELISA.**

| Group | Days post immunization | | | | | |
|---|---|---|---|---|---|---|
| | 0 | 7 | 14 | 21 | 28 | 35 |
| pcDNA3.1/H5 | 0/9* | 0/9 | 0/9 | 2/9 | 3/9 | 5/9 |
| pcDNA3.1/H5 + pcDNA3.1/ MDP1 | 0/9 | 0/9 | 2/9 | 4/9 | 5/9 | 8/9 |
| pcDNA3.1/ MDP1 | 0/9 | 0/9 | 0/9 | 0/9 | 0/9 | 0/9 |
| pcDNA3.1 + | 0/9 | 0/9 | 0/9 | 0/9 | 0/9 | 0/9 |
| Negative control | 0/9 | 0/9 | 0/9 | 0/9 | 0/9 | 0/9 |

* The ratio of positive treatments to the inoculated chickens

nized with H5 + MDP1 vaccines were higher than mean HI titers recorded from chickens immunized with H5 vaccine. However, the HI titers for both groups never exceeded 16. The highest average antibody titers were detected one week after the second booster, at day 35 post immunization of 13.33 ± 4.13 in chickens immunized with H5 + MDP1 vaccines, as shown in Table 4. Thus, higher antibody titer were observed in chickens immunized with H5 + MDP1 vaccines, compared to chickens immunized with H5 vaccine at day 14, 21, 28 and 35 post vaccination (Table 4). However, the HI titer increase was not statistically significant. As expected, the chickens immunized with pcDNA3.1, pcDNA3.1/MDP1, normal saline and left unimmunized failed to demonstrate detectable HI titer (Table 4).

### Reverse Transcription-Polymerase chain reaction

The ability of the constructed H5 and MDP1 vaccines in inducing mRNA expression for H5 and MDP1 was studied using RT-PCR following intramuscular immunization of the SPF chickens, respectively. Bands of the expected size (141 bp) indicative of H5 transcripts were detected from the spleen and muscle samples of the H5 and H5 + MDP1 immunized groups (Figure 2). Additionally, the expression of MDP1 constructed plasmid was confirmed in groups immunized with MDP1 + H5 and MDP1 alone

**Table 4: Mean hemagglutinin inhibition (HI) results of serum samples from immunized chickens.**

| Group | Days post immunization | | | | |
|---|---|---|---|---|---|
| | 7 | 14 | 21 | 28 | 35 |
| pcDNA3.1/H5 | ND (0/9)* | 0.67 ± 1.03 (2/9) | 2.33 ± 0.82 (6/9) | 5 ± 2.45 (9/9) | 10.67 ± 4.13 (9/9) |
| pcDNA3.1/H5 + pcDNA3.1/MDP1 | ND (0/9) | 0.83 ± 0.98 (2/9) | 3.33 ± 2.42 (7/9) | 9.33 ± 5.46 (9/9) | 13.33 ± 4.13 (9/9) |
| pcDNA3.1/MDP1 | ND (0/9) | ND(0/9) | ND(0/9) | ND(0/9) | ND(0/9) |
| pcDNA3.1 | ND (0/9) | ND(0/9) | ND(0/9) | ND(0/9) | ND(0/9) |
| Negative control | ND (0/9) | ND(0/9) | ND(0/9) | ND(0/9) | ND(0/9) |

ND: Not detected

* The ratio of positive treatments to the inoculated chickens